IEEE Access
Multidisciplinary ⋮ Rapid Review ⋮ Open Access Journal

Received March 21, 2021, accepted April 2, 2021, date of publication April 12, 2021, date of current version April 19, 2021.

Digital Object Identifier 10.1109/ACCESS.2021.3072360

Observers for High-Speed Sensorless PMSM Drives: Design Methods, Tuning Challenges and Future Trends

CESAR JOSÉ VOLPATO FILHO[1], DIANXUN XIAO[2], (Student Member, IEEE), RODRIGO PADILHA VIEIRA[1], (Member, IEEE), AND ALI EMADI[2], (Fellow, IEEE)

[1]Power Electronics and Control Research Group, Federal University of Santa Maria, Santa Maria 97105-900, Brazil
[2]McMaster Automotive Resource Center (MARC), McMaster University, Hamilton, ON L8P 0A6, Canada

Corresponding author: Dianxun Xiao (xiaod6@mcmaster.ca)

This work was supported in part by the Natural Sciences and Engineering Research Council of Canada (NSERC), and in part by the Coordenação de Aperfeiçoamento de Pessoal de Nível Superior—Brasil (CAPES/PROEX)—Finance Code 001.

ABSTRACT Rotor position and speed estimation methods are consolidated to reduce the cost and volume of permanent magnet synchronous motor (PMSM) sensorless control drives while maintaining high performance. Advanced nonlinear algorithms require accurate design for precise estimation tracking throughout the entire PMSM operation range. This paper presents a broad review of the main high-speed estimation methods for sensorless PMSM drives. First, the stability constraints and design methodologies of the main estimation techniques presented in the literature are discussed. In the second part, it is investigated the new observer design trends, which are used under non-ideal conditions, such as robustness to distortions, the effects of parameter variation, sensorless parameter estimation, and low sampling-frequency-to-speed ratio operation. Future trends on the design of observers for high-speed sensorless PMSM drives are also discussed.

INDEX TERMS High performance drives, permanent magnet synchronous motors, sensorless control, state observer design.

I. INTRODUCTION

Permanent magnet synchronous motors (PMSMs) have been extensively used in modern electrical drives due to their high performance. The higher efficiency and higher power density are the major assets of the PMSM in relation to its main competitor, the induction motor. Furthermore, closed-loop control requires accurate position information of the PMSM. This mechanical information can be extracted through an encoder or a resolver, which is expensive and bulky. Since the disadvantages are unwanted, sensorless control techniques have been a major topic of study [1], [2]. The rotor position estimation techniques are mainly classified into two categories, low-speed methods and high-speed methods. The low-speed sensorless approach depends upon high-frequency injection for computation of the position information through the motor reluctance. An in depth review of high frequency based estimation for low-speed sensorless PMSM drives is performed in [3]. The high-speed methods are based on the computation of the PMSM flux or electromotive force, which is directly related to the rotor position.

The first high-speed sensorless control methods for PMSMs were presented in the 1970s and 80s and were based on open-loop strategies [4]–[7]. These approaches are sensitive to model mismatches, measurement errors and have poor dynamic behavior. In order to improve the estimation performance from the open-loop algorithms, nonlinear observer techniques began to be investigated in the following decades [8]–[12]. Such methods make use of feedback for expansion of the system robustness, which can lead to faster estimation tracking. However, the first publications with these strategies were a direct application of the theoretical methods, which were mainly focused on the observer stability for high-order nonlinear systems. In sensorless applications, fast estimation of the mechanical variables is required to ensure that the closed-loop control will be not significantly affected. Therefore, it is necessary to adjust the design methods of high-order nonlinear observer techniques for the PMSM sensorless application, which requires, in addition to stability, good dynamic estimation performance.

The associate editor coordinating the review of this manuscript and approving it for publication was Zhong Wu.

TABLE 1. PMSM linear models in the stationary frame.

Model	x	A	B	C	u
Linear Flux	$\begin{bmatrix} i \\ \lambda \end{bmatrix}$	$\begin{bmatrix} -I\frac{R}{L_q} & -\frac{J\omega_e}{L_q} \\ 0 & J\omega_e \end{bmatrix}$	$\begin{bmatrix} \frac{I}{L_q} \\ 0 \end{bmatrix}$	$\begin{bmatrix} I & 0 \end{bmatrix}$	v
EEMF	$\begin{bmatrix} i \\ e \end{bmatrix}$	$\begin{bmatrix} -I\frac{R}{L_d}+J\omega_e\frac{L_d-L_q}{L_d} & -\frac{I}{L_d} \\ 0 & J\omega_e \end{bmatrix}$	$\begin{bmatrix} \frac{I}{L_d} \\ 0 \end{bmatrix}$	$\begin{bmatrix} I & 0 \end{bmatrix}$	v

The most advanced estimation techniques require an adequate adjustment of the observer feedback gains. A wide range of studies from the last decade seeks to synthesize the observer gains in closed-form solutions, which can be generalized for all PMSMs. Another focus of recent research efforts is developing additional observer analysis tools and improving the observer performance under nonideal conditions. Such topics include the analysis of PMSM parameter variation effects, online parameter estimation, and position observer design against distortions. The study of high speed sensorless applications with low sampling frequencies has also received attention.

This paper presents a comprehensive review on the design of rotor position estimation methods for high-performance sensorless control of PMSM drives. In Section II, the established observer techniques, their design procedures, and performance specifications are discussed. The effects of parameter variation on the position estimation, parameter estimation algorithms, harmonic and dc error suppression through observer modification, and low sampling frequency to speed ratio observer design are investigated in Section III. The future work on position observer design is discussed in Section IV. Finally, the conclusion of the paper is presented in Section V.

II. OBSERVER DESIGN FOR HIGH PERFORMANCE POSITION AND SPEED ESTIMATION

High-performance position and speed estimations are essential for the field-oriented sensorless control, a typical sensorless control diagram is presented in Fig. 1. If slow estimation occurs, the closed-loop speed control can become unstable, and the field orientation can be lost. In the case of too high observer bandwidth, the estimation algorithm can amplify the measurement noise, which can lead to additional torque loses. Therefore, the design properties are essential in the PMSM sensorless control system performance. In this section, the major PMSM observer design issues, such as models, control techniques, and gain design, are presented.

A. PMSM MODEL

Model-based estimation algorithms have been the main approach for sensorless control of PMSM drives in the medium and high-speed range [13]. The mathematical model of the PMSM is generally defined by the stator current equations in the synchronous frame [14] and is given by

$$\boldsymbol{v}_{dq} = \boldsymbol{L}_{dq}\rho\boldsymbol{i}_{dq} + R\boldsymbol{i}_{dq} + \boldsymbol{J}\boldsymbol{L}_{dq}\omega_e\boldsymbol{i}_{dq} + \boldsymbol{g}\omega_e\psi, \qquad (1)$$

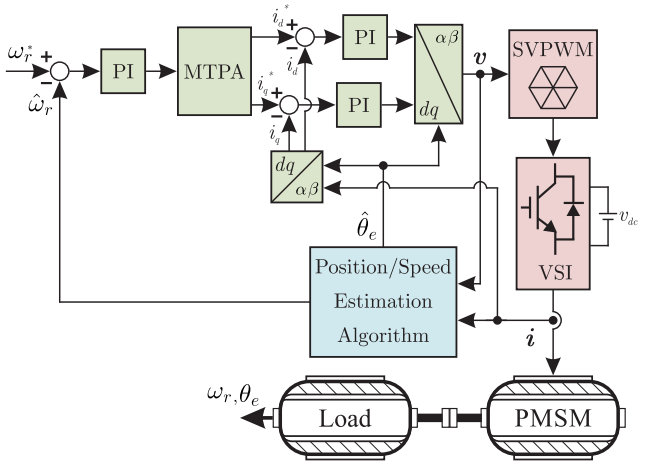

FIGURE 1. Field oriented PMSM sensorless control diagram.

where

$\boldsymbol{i}_{dq}$ stator current vector in the synchronous frame,
$\boldsymbol{v}_{dq}$ stator voltage vector in the synchronous frame,
L_d, L_q stator inductances,
R stator resistance,
ω_e, ω_r rotor flux speed and rotor speed,
ψ permanent magnet flux linkage,
ρ differential operator,

$$\boldsymbol{L}_{dq} = \begin{bmatrix} L_d & 0 \\ 0 & L_q \end{bmatrix}, \boldsymbol{g} = \begin{bmatrix} 0 \\ 1 \end{bmatrix}.$$

In the stationary reference frame, the most popular representations of the PMSM dynamics are the linear flux $\boldsymbol{\lambda}$ [15] and the extended electromotive force (EEMF) $\boldsymbol{e}$ [16].Both modeling approaches create vectors oriented with the PMSM rotor and have an angle equal to the rotor flux position θ_e. Other less popular models are also presented in the literature [17], [18].

The attractiveness of EEMF and linear flux models are the ability to create linear models where the established control techniques and analysis methods can be easily implemented. The linear flux and EEMF models are represented in the linear form

$$\begin{cases} \dfrac{d}{dt}\boldsymbol{x} = \boldsymbol{A}\boldsymbol{x} + \boldsymbol{B}\boldsymbol{u} \\ \boldsymbol{y} = \boldsymbol{C}\boldsymbol{x} \end{cases} \qquad (2)$$

and in Table 1, where $\boldsymbol{v}$ and $\boldsymbol{i}$ are the stator voltage and current vectors in the stator frame, respectively,

$$\boldsymbol{I} = \begin{bmatrix} 1 & 0 \\ 0 & 1 \end{bmatrix}, \boldsymbol{J} = \begin{bmatrix} 0 & -1 \\ 1 & 0 \end{bmatrix}, \boldsymbol{0} = \begin{bmatrix} 0 & 0 \\ 0 & 0 \end{bmatrix}.$$

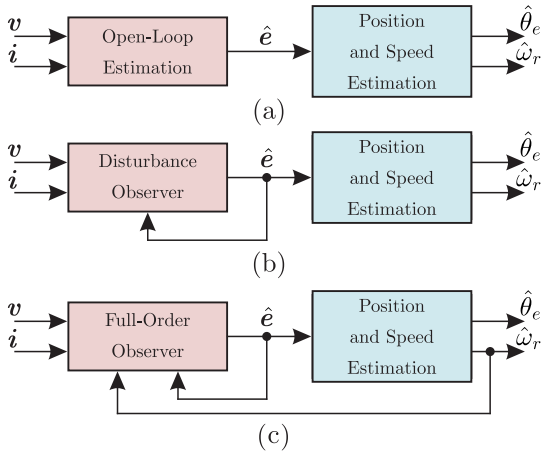

FIGURE 2. Main PMSM estimation approaches: (a) Open-Loop (b) Disturbance observer (c) Full-order observer.

The EEMF and linear flux accurately represent the behavior of the salient pole PMSM. Furthermore, when $L_q = L_d$, the EEMF, which becomes the standard electromotive force [19], and the linear flux [20] models both describe the non-salient pole PMSM. Although it does not present magnets in its rotor, the synchronous reluctance motor can also be represented by such models. In order to simplify the paper representation, the EEMF is used in equations and figures.

The observability properties of the PMSM model, studied in [21]–[23], indicate that position estimation process at low speeds can only be performed using the insertion of high-frequency signals [24]–[31]. In the case of the surface PMSM (SPMSM), even with the insertion of high-frequency components, the position estimation can be a difficult task [32]. The characteristic of observability deficiency at low speeds of the PMSM can be explained by the difficulty of extracting the EEMF vector angle when its value is null. In the case of the linear flux model, the term $\boldsymbol{J}\omega_e\boldsymbol{\lambda}$ is equal to zero when the rotor is at standstill, making it impossible to observe the rotor flux, and consequently, the position information is unreachable.

The linear model (2) fits the traditional control design problems. Three main estimation methodologies stand out in the literature for the observer design. The first computes the EEMF directly by the PMSM equations. This strategy, known as open-loop estimation, is susceptible to unmodeled dynamics and rapidly fell into disuse. The second most popular strategy is to use an observer with the same order as the plant; that observer is known as a full-order observer [33]. This method contains the multiplication of the estimated EEMF and speed, which implies high design complexity. The third major estimation method category uses the disturbance observer technique [34] in order to eliminate the full-order observer nonlinearities. Through the disturbance observer, the coupling between the stationary axes disappears since the EEMF, where the coupling takes place, is modeled as a disturbance. These three prevalent strategies are illustrated in Fig. 2. Position and speed reconstruction algorithms

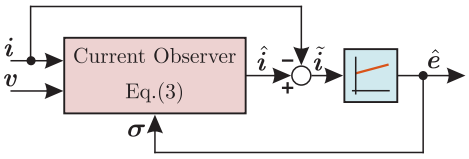

FIGURE 3. Linear disturbance observer block diagram.

are required to extract the mechanical variables from the observed EEMF. If the position and speed are observed states from the full-order observer, the reconstruction procedure is not required.

B. DISTURBANCE BASED OBSERVER

The disturbance observer is developed through the stator current equations of the PMSM model, such as

$$\frac{d}{dt}\hat{\boldsymbol{i}} = \boldsymbol{\rho}_1(\boldsymbol{u}, \boldsymbol{x}, t) + \boldsymbol{\sigma} \tag{3}$$

where $\boldsymbol{\rho}_1(\boldsymbol{u}, \boldsymbol{x}, t)$ is the perturbation term, which is dependent on the PMSM model, and $\boldsymbol{\sigma}$ is the observed disturbance, which estimates the EEMF vector. By selecting the perturbation term $\boldsymbol{\rho}_1(\boldsymbol{u}, \boldsymbol{x}, t)$ according to the PMSM model with the exception of the EEMF, the observed disturbance will achieve good tracking of the EEMF if the observed current converges to the actual one.

The main advantage of the disturbance observer estimation strategy is to avoid the nonlinearities of the full-order observer. Thus, the design of the estimator is broken in two simple systems, a disturbance observer and a position and speed reconstruction method.

1) LINEAR DISTURBANCE OBSERVER

The simplest topology of the disturbance observer approach is the linear disturbance observer (LDO) [35]–[37]. This strategy design the observed disturbance as a linear feedback variable, enabling the use of classic control tools, such as bode diagram, as an analysis tool. The observed disturbance is defined as

$$\boldsymbol{\sigma} = \boldsymbol{\rho}_2(\boldsymbol{u}, \boldsymbol{x}, t)\,\tilde{\boldsymbol{i}}, \tag{4}$$

where $\boldsymbol{\rho}_2(\boldsymbol{u}, \boldsymbol{x}, t)$ defines the linear magnitude and frequency responses of the LDO. The block diagram of the LDO method is illustrated in Fig. 3.

The main disadvantage of the LDO is the uneven behavior in relation to the frequency of operation, which alters the performance of the estimator significantly in applications with high speed range. Furthermore, the absence of the EEMF dynamics in the perturbation design leads to higher bandwidth requirements for acceptable dynamic performance, which results in noise sensitivity.

2) SLIDING MODE DISTURBANCE OBSERVER

The pursuit for proper EEMF tracking through the entire PMSM operating range by the disturbance method culminated in the study of sliding mode observer (SMO)

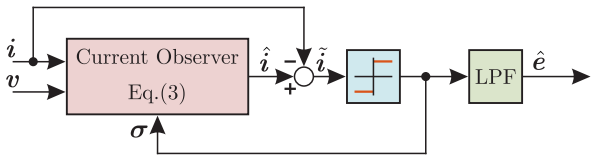

FIGURE 4. Sliding mode disturbance observer block diagram.

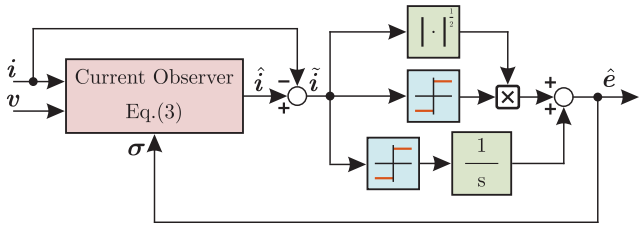

FIGURE 5. Super-twisting sliding mode disturbance observer block diagram.

strategies [38]–[44]. The sliding mode technique uses a high-frequency switching variable in order to ensure robustness to the observation process. The observed sliding mode disturbance is defined as follows:

$$\boldsymbol{\sigma} = k_1 sign\left(\tilde{\boldsymbol{i}}\right), \tag{5}$$

where k_1 is the SMO gain. If k_1 is designed high enough, sliding is guaranteed and, therefore, EEMF tracking. The block diagram of the SMO strategy is presented in Fig. 4.

The SMO approach is one of the most popular sensorless PMSM control methods. This is due to the easy design of the high-frequency switching variable and straightforward implementation. On the other hand, the resulting observed EEMF by the high-frequency component contains excessive noise, known in the literature as the chattering phenomenon, which makes the direct use of SMO unwanted. Thus, the filtering of the observed high-frequency variable is desired, which reduces the chattering in the observed EEMF.

Filtering of the SMO disturbance leads to phase deviation of the observed EMF, thus requiring phase adjustments. In order to avoid this corrections, the replacement of the sign function by the sigmoid function can be performed [45]. This substituting eliminates the chattering phenomenon from the SMO but removes the sliding feature of the algorithm.

In order to avoid the chattering reduction procedure from the standard SMO, the super-twisting sliding mode algorithm, which was developed in [46], was investigated [47]–[51]. The observed disturbance of the super-twisting observer (STO) is defined as

$$\boldsymbol{\sigma} = k_2 \left|\tilde{\boldsymbol{i}}\right|^{\frac{1}{2}} sign\left(\tilde{\boldsymbol{i}}\right) + \int k_3 sign\left(\tilde{\boldsymbol{i}}\right) dt \tag{6}$$

where k_2 and k_3 are the STO gains. The overall structure of the STO method is illustrated in Fig. 5.

In the STO strategy, while the standard high-frequency switching variable ensures that the observed EEMF will slide the actual ones, the chattering effect is reduced by the new integral portion part. The major drawback of the super-twisting approach is the design of k_2 and k_3 due to the discontinuous dynamics of the system, which are difficult to model and analyze.

C. FULL-ORDER OBSERVER

The rotor position estimation can be achieved by the full-order observer method, which implements the complete PMSM model with the addition of feedback. In this approach, the EEMF is viewed as a state and not as a disturbance, reducing the high bandwidth requirement in comparison with the LDO. Furthermore, the speed dependent full-order observer poles can be easily extracted, which allows an easy variable gain design for wide speed range applications.

1) FULL-ORDER OBSERVER IN STATIONARY FRAME

Rotor position and speed estimation can be achieved by the extension of the classical Luenberger observer [52]. The full-order observer (FOO) is built through the PMSM linear models, given in Table 1, such as follows

$$\begin{cases} \dfrac{d}{dt}\hat{\boldsymbol{x}} = \hat{\boldsymbol{A}}\hat{\boldsymbol{x}} + \boldsymbol{B}\boldsymbol{u} + \boldsymbol{H}\left(\hat{\boldsymbol{y}} - \boldsymbol{y}\right) \\ \hat{\boldsymbol{y}} = \boldsymbol{C}\hat{\boldsymbol{x}} \end{cases} \tag{7}$$

where $\boldsymbol{H}$ is the feedback gain matrix, $\hat{}$ and $\sim$ express the estimated variables and the error between the estimated variables and the actual variables, respectively.

The good performance of the FOO, required for accurate position tracking, depends on the adjustment of the gain matrix $\boldsymbol{H}$. Such design is performed through the error dynamics of the FOO, which can be obtained by subtracting (2) from (7), such as

$$\frac{d}{dt}\tilde{\boldsymbol{x}} = \boldsymbol{A}'\tilde{\boldsymbol{x}} + \boldsymbol{B}'\hat{\boldsymbol{x}}\tilde{\omega}_e \tag{8}$$

where $\boldsymbol{A}' = \boldsymbol{A} + \boldsymbol{H}\boldsymbol{C}$ and $\tilde{\omega}_e\boldsymbol{B}' = \tilde{\boldsymbol{A}}$.

The non-linear characteristic of the PMSM model is highlighted in (8), where the rotor speed, which is unknown in a sensorless operation, directly impacts the poles of $\boldsymbol{A}'$. Hence, for a fixed $\boldsymbol{H}$, the estimation convergence will be dependent on the PMSM operating point, which will lead the observer to have poor estimation performance and may even cause instability in the sensorless control system. In order to solve this problem, the FOO design methods converge in using the estimated speed in the feedback matrix $\boldsymbol{H}$, which linearizes the estimation behavior of the observer. Through this design configuration, the poles of $\boldsymbol{A}'$ can be adjusted by pole placement, H_∞ and LMI techniques [53]–[56]. These design methods are only ideal when the estimated speed matches the actual one. When speed estimation error occurs, the observer poles diverge from the designed positions, which may lead the system to instability.

The FOO stability conditions are studied in [57], where positive real conditions for arbitrary speed estimation algorithm are obtained by applying the Kalman-Yakubovich Lemma (KYL) to the observer error equations (8), such as

$$\begin{cases} \boldsymbol{A}'^{T}\boldsymbol{P} + \boldsymbol{P}\boldsymbol{A}' \leq \boldsymbol{0} \\ \boldsymbol{P}\boldsymbol{B}' = \boldsymbol{C}^{T} \end{cases} \tag{9}$$

where $^{\exists}\boldsymbol{P} = \boldsymbol{P}^{T} > \boldsymbol{0}$.

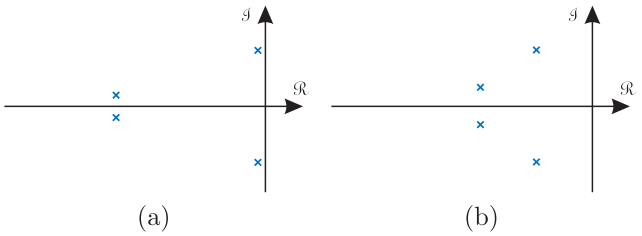

FIGURE 6. FOO normalized poles (a) poorly damped design (b) improved pole placement design.

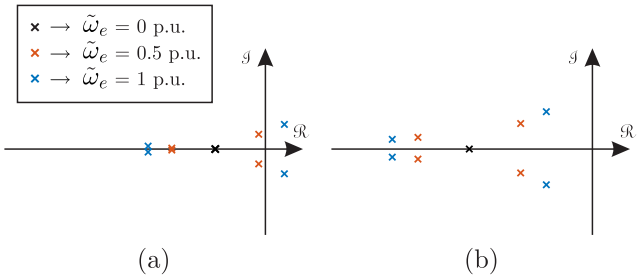

FIGURE 7. FOO poles with cascade design and (a) lower bandwidth (b) higher bandwidth.

The feedback gains derived from the KYL (9), which are dependent on the actual rotor speed, stabilize the FOO for arbitrary adaptive speed estimator gains. Furthermore, it is shown in [57] that the local stability is still guaranteed when the estimated speed is used for the implementation of the stabilization gains. Such feedback gain design however, can lead to a poorly damped performance, which can force the control system to instability at sensorless operation, especially under load conditions. The normalized poles of a poorly damped designed FOO is presented in Fig. 6 (a). It is highlighted that small speed estimation errors can move the FOO poles to the real axis. Thus, it is shown that the a pole placement assignment can improve the FOO damping and robustness. The FOO normalized poles with improved pole placement estimation is showed in Fig. 6 (b).

The damping design approach can be unintuitive, since the relationship between the FOO gains and the estimation error is not addressed in the stability analysis. In [58], a cascade design strategy is presented in order to make the gain tuning process intuitive. In this design method, the state observer operates at higher frequencies, which demonstrates increasing the observer robustness to speed estimation errors. The adaptive speed estimation law is configured at lower frequencies, thus facilitating the modeling of the FOO gains. The FOO pole behavior under speed estimation error is shown in 7 (a). As speed estimation error is increased, the FOO eventually becomes unstable. The effect of increasing the FOO bandwidth on the robustness is illustrated in 7 (b). By moving the poles further to the left of the real axis, the effect of speed estimation error is mitigated and the robustness is increased. The cascade design concept, where the state observer is arranged with high bandwidth for expanded robustness, is mainly limited by the sampling frequency.

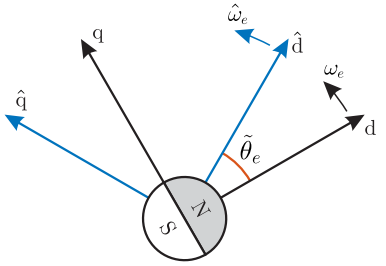

FIGURE 8. Full-order observer vector diagram in the synchronous frame.

Despite the FOO stability is intrinsically dependent on the PMSM actual speed, the design approaches [57], [58] ensure robustness to high speed estimation errors. Moreover, the variable feedback gains linearize the estimation behavior in relation to the PMSM speed. It is opposite to the LDO, which has an uneven frequency response, and the SMO, which the chattering is dependent on the operation point.

2) FULL-ORDER OBSERVER IN SYNCHRONOUS FRAME

The FOO can be built in the synchronous rotating frame [59]–[63] through the model (1), such as

$$\boldsymbol{L}_{dq}\rho\hat{\boldsymbol{i}}_{dq} = \boldsymbol{v}_{dq} - R\hat{\boldsymbol{i}}_{dq} - \boldsymbol{J}\boldsymbol{L}_{dq}\hat{\omega}_e\hat{\boldsymbol{i}}_{dq} - \boldsymbol{g}\hat{\omega}_e\psi + \boldsymbol{H}_{dq}\tilde{\boldsymbol{i}}_{dq} \tag{10}$$

where $\boldsymbol{H}_{dq}$ is the observer feedback gain matrix in the synchronous frame.

In the rotating reference, it is not possible to guarantee that the currents and voltages measured in the synchronous reference are correct, since the estimated position is used in the Park transformations and can lead to a phase error in the observed synchronous variables. Thus, despite the observer having a lower order in the rotating frame, the FOO in the synchronous frame is affected by both the speed and position estimation errors, while the FOO in the stationary frame is only affected by speed estimation error. The FOO vector diagram in the synchronous frame is illustrated in Fig. 8. The stability and convergence analysis of the FOO in the rotating frame can be accurately modeled by the linearization of the observer error dynamics as a function of position and speed estimation errors [62], which is given by

$$\frac{d}{dt}\begin{bmatrix}\tilde{\boldsymbol{i}}_{dq}\\ \tilde{\theta}_e\end{bmatrix} = \boldsymbol{A}_{dq}\begin{bmatrix}\tilde{\boldsymbol{i}}_{dq}\\ \tilde{\theta}_e\end{bmatrix} + \boldsymbol{B}_{dq}\tilde{\omega}_e \tag{11}$$

where $\boldsymbol{A}_{dq}$ and $\boldsymbol{B}_{dq}$ are the observer error state and input matrices, respectively.

The design of the poles of $\boldsymbol{A}_{dq}$, which is dependent on the actual speed, has similar obstacles as the design of $\boldsymbol{A}'$. Variable speed-dependent feedback gain $\boldsymbol{H}_{dq}$ can improve the estimation performance, and damping enhancement is required. One explicit conclusion from the error equation (11) is that, if the observer closed-loop poles are properly designed, good rotor position estimation is accomplished. Therefore, the estimated rotor position can be obtained through the integration of the rotor flux speed, since the

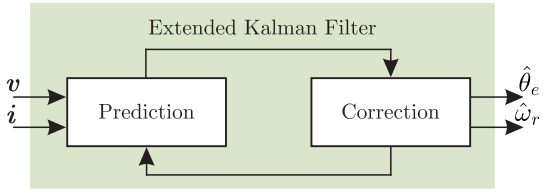

FIGURE 9. EKF based estimation structure.

estimation structural guarantee the field orientation. In the case of the observer in the stationary frame, the integration of the rotor speed for position estimation can lead to the integration shift phenomenon [64].

The equivalence between the FOO in the stationary and synchronous frame is presented in [57].

3) EXTENDED KALMAN FILTER ESTIMATION

The FOO approach presented in the previous subsections requires a gain design procedure, which are limited to the design conditions previously defined. In contrast with such techniques, the extended Kalman filter (EKF) is a near to optimal estimation algorithm, where feedback gains are recalculated constantly. This characteristic makes it known as the standard of nonlinear systems estimation. The EKF is used in PMSM sensorless applications in [65]–[71]. The EKF algorithm is composed by two main steps: Prediction and Correction, which are illustrated in Fig. 9 and summarized as follows:

1) ***Prediction***: The observed vector $\hat{\boldsymbol{x}}^{ekf} = \begin{bmatrix} \hat{\boldsymbol{i}} & \hat{\theta}_e & \hat{\omega}_e \end{bmatrix}^T$ is computed through the stator currents and voltages similarly to an open-loop method. The covariance matrix $\boldsymbol{P}$ is predicted using the noise covariance matrix $\boldsymbol{Q}$, which needs to be tuned, and the Jacobian matrix of the PMSM model.
2) ***Correction***: The near-optimal feedback gain $\boldsymbol{H}^{ekf}$, which is known to produce fast estimation, is computed and used to correct and observe the estimated variables. The measurement noise covariance matrix $\boldsymbol{R}$ is a tuning variable of the feedback gain calculation. Correction of the covariance matrix is also performed. The estimation of the correction EKF step is performed by the following relationship

$$\hat{\boldsymbol{x}}_k^{ekf} = \hat{\boldsymbol{x}}_{k-1}^{ekf} + \boldsymbol{H}^{ekf}\tilde{\boldsymbol{i}} \tag{12}$$

The near to optimal performance of the EKF is not obtained without disadvantages. The covariance matrices $\boldsymbol{R}$ and $\boldsymbol{Q}$ are complex to design [72] and generally are determined empirically. Such determination is inadequate for PMSM drives built for an extensive range of motors, for which parameters are not known previously. Thus, the estimation algorithms presented in the previous subsections, which synthesize the observer gains in closed-form solutions and are easily applicable for general-purpose PMSM drives, have a leverage in this situation. Furthermore, the calculation of the Jacobian matrix lead to a significant larger computational cost in comparison with the other estimation methods. These

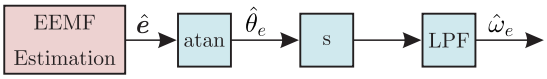

FIGURE 10. Speed estimation through derivative method.

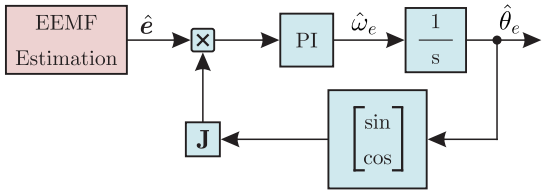

FIGURE 11. PLL for position and speed reconstruction.

characteristics, of high computational cost and difficulty in designing the covariance matrices, overcome the near to optimal feature of the EKF, making it an unattractive option in the majority of the situations.

A summarized table of the main characteristics of the major position estimation methods is given in Table 2.

D. ROTOR POSITION AND SPEED RECONSTRUCTION METHODS

In order to fulfill the estimation algorithm, the PMSM position and speed must be reconstructed from the observed EEMF obtained from the disturbance or full-order observer. The most popular position and speed computation strategies are the derivative approach, the phase-locked loop (PLL) method, and the adaptive algorithm.

The derivative approach [47], [48], [50], which is the most straightforward and is showed in Fig. 10, computes the rotor position from the angle of the observed EEMF/flux by a trigonometric function, and the rotor speed is obtained by the derivative of the estimated position. Speed filtering is necessary due to the derivative function.

Position reconstruction can also be performed by the PLL method [38], [39], [74], which is illustrated in Fig. 11. In this algorithm, the estimated rotor speed is an internal variable. The PLL creates an adjustable vector with variable angle and compares with the observed disturbances. When the error between the vector is small, good position estimation is obtained. The proportional-integral (PI)-type regulator is usually used to converge the observed position, and its design is easy due to the PLL modeling simplicity. Furthermore, the PLL has a broad use in electrical power systems, thus being already well known by many designers.

Another major reconstruction method for the mechanical variables is the adaptive approach [41], [73], that is demonstrated in Fig. 12. This strategy makes use of the gradient descendent algorithm with an adjustable model in order to track the frequency of the observed EEMF. The adaptive method requires design of internal feedback gains for the adjustable model and the gradient descendent adaptive gains. Both feedback and adaptive gains offer additional filtering properties, key features of the adaptive algorithm. The adaptive approach can also be integrated with the FOO

TABLE 2. Summary and comparison of the major position estimation methods for sensorless PMSM drives.

Position Estimation Category	Observer Method	Convergence Rate	Stability Constraints	Gain Design Complexity	Advantages	Disadvantages
Open Loop Estimation [4]–[7]	None	Low	High	None	No tunable parameters	Susceptible to measurement disturbances, slow dynamic response, poor robustness
Disturbance Observer	LDO [35]–[37]	Medium	Medium	Low	Simple implementation	Frequency variant performance
	SMO [38]–[43], [74] STO [47]–[51]	High	Low	Low	Fast convergence and robustness	Chattering problem, complex high-order SMO gain design
Full-Order Observer	Luenberger [57]–[62]	High	Medium	Medium	Uniform performance	Stability dependency on the actual rotor speed value
	Extended Kalman Filter [65]–[71]	High	Low	High	Anti-measurement noise capability	Complex design of the covariance matrices, computional burden

[57], [58], where FOO itself is the adjustable model, making it an adaptive full-order observer.

III. OBSERVER DESIGN FOR HIGH PERFORMANCE ESTIMATION UNDER NON-IDEAL CONDITIONS

In the previous section, the major state observer design strategies for high performance sensorless control are investigated. The analysis and design of these schemes consider an ideal system, where current and voltage measurement inaccuracies, inverter nonlinearities, sampling limitations, and parameter variations are not taken into account. Recent research efforts seek to model such PMSM sensorless control system issues and propose modifications on the observer topologies, which require new design methodologies.

In this section, the main observer design methods under non-ideal conditions, which aim to improve position and speed estimation tracking, are presented.

A. LOW SAMPLING-FREQUENCY-TO-SPEED RATIO

Modern PMSM sensorless control algorithms are implemented through digital systems. In cases where the sampling frequency f_{samp} is very low in relation to the PMSM rotor flux fundamental frequency f_{ω_e}, the observer design methods presented in Section II may have inadequate estimation performance or even may become unstable, making them unsuitable as a sensorless control algorithm.

In [75] a designed method for the FOO in the synchronous frame in the discrete-time domain is proposed. It is demonstrated that the inherently delays in the control system, which can be addressed in discrete-time, affect the observer performance. The proposed design methodology is compared experimentally to the FOO designed in the continuous-time using the forward Euler approximation. The sampling-frequency-to-speed ratio was $f_{ratio} = f_{samp}/f_{\omega_e} = 10$ for the proposed method, which presented good response, and $f_{ratio} = 30$ for the FOO designed in the continuous-time, which became unstable. It is shown that major performance improvements can be obtained by the design in the discrete-time. Similar results are obtained in [76], where the observer aims to compensate the voltage error caused by delay. The advantages of the discrete-time design over the standard discretized FOO are demonstrated, and a $f_{ratio} = 10$ is achieved experimentally. The importance of delay compensation under low-frequency sampling is demonstrated in [77]. When the delay is not compensated, the position estimation error appears as rotor speed increases, with a linear relationship. This estimation error can be almost eliminated by digital delay compensation. Under $f_{ratio} = 10$ experimental results are presented [78]–[80] with no-load operation and, when shaft load is applied to the PMSM, lower f_{ratio} is achieved. These results suggest that the observer robustness in discrete-time is dependent on the PMSM load. This can be due to parameter error that arises due to inductance saturation at high currents. However, analytical analysis on the observer robustness degradation in discrete-time under load operation is still missing.

The SMO technique applied for low f_{ratio} operation is also studied [81], [82]. In discrete-time domain, the sliding property of the SMO is not valid, and only quasi-sliding mode observation can be achieved [83]. Furthermore, under low f_{ratio}, the chattering phenomenon increases, and its reduction is of great importance. In [73] the chattering is reduced by two lowpass filters, one internal in the SMO and other after the EEMF is observed. Phase compensation due to the filtering process is required. Bandpass filter can also be employed in order to reduce the SMO chattering. This strategy does not require phase compensation since the bandpass filter is a zero phase-shift amplifier [81].

The discretization method is crucial in order to achieve high performance low f_{ratio} estimation. The FOO observer poles with exact discretization, Euler and Tustin approximations are compared in [79] and are illustrated in Fig. 13. As the PMSM rotor speed increases, the observer poles move further to the left plane of the real axis. When the Euler approximation is employed, the estimation becomes highly oscillatory at high speeds. The Tustin approximation does not

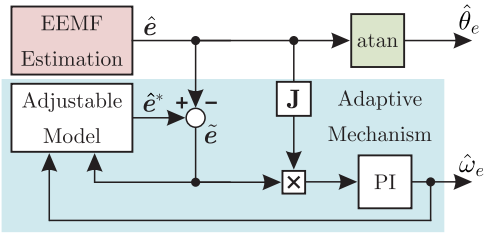

FIGURE 12. Adaptive approach for position and speed estimation.

exhibit oscillatory behavior of the Euler method but suffers from degradation in performance compared to the exact discretization.

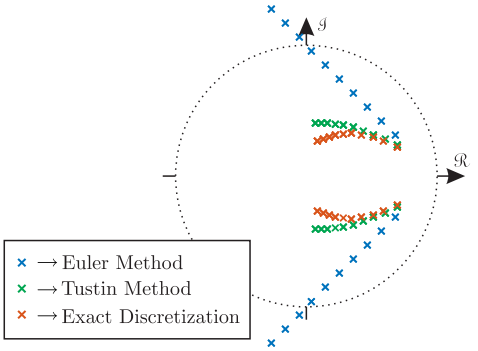

FIGURE 13. Discrete-time poles as bandwidth increase with different discretization methods.

B. MOTOR-PARAMETER-ADAPTIVE POSITION OBSERVER

1) EFFECTS OF PARAMETER VARIATION

High-performance position-sensorless control of PMSMs relies on accurate motor parameters, such as stator resistance, stator inductance, and magnetic flux linkage. Fundamental-frequency-based methods, available at medium and high speed, are considered to be more sensitive to parameter mismatch due to the motor model dependence [84]. For low-speed sensorless control, signal-injection-based schemes are motor-parameter-independent, while the accurate motor parameters are still expected for robust current/torque control performance [85]. Generally, model sensitivity in position estimation is only analyzed on model-based techniques, such as EEMF-based methods [45] and stator flux-based methods [61]. Regardless of which the estimation model is adopted, the parameter sensitivity characteristics would be identical. In [52], the stator resistance and inductance mismatch effects on position estimation of an SPMSM are discussed. The steady-state analysis illustrates that a phase shift is generated in the estimated EEMF due to the parameter deviation and results in a position estimation offset. In [86], a more general solution in parameter sensitivity of both SPMSMs and IPMSMs is proposed adopting a sensitivity function. This technique can quantitatively investigate the steady-state parameter sensitivity, and the analytical result of the EEMF-based position estimation is presented in Fig. 14. Intuitively, the sensitivity function of the q-axis inductance is largest, showing the q-axis inductance can lead to a dominant position estimation error, and the adverse effect is speed-independent. The stator resistance influence is less and is reduced at a higher speed. In contrast, the d-axis inductance mismatch and flux linkage mismatch have null sensitivity functions in the EEMF-based estimation, which means the estimator is insensitive to these two parameters.

For accurate position estimation, the q-axis inductance and stator resistance need to be accurate. Although the d-axis inductance and flux linkage have no effects on steady-state estimation accuracy, accurate d-axis inductance is essential for robust current controller design, and the flux linkage can be used for temperature estimation in a high-power PMSM. The nominal parameters of a PMSM are typically given by manufacturers and are available for basic position observer design, but the motor parameters vary with ambient temperature and stator current [87]. For instance, high temperature can result in increasing stator resistance and demagnetizing flux linkage. Magnetic saturation is aggravated at high current levels (i.e., load conditions), leading to decreased stator inductance. However, there are some limits of measuring motor parameters under driving conditions, especially for the stator resistance and flux linkage that are temperature-dependent since the stator and rotor temperature measurement is hard in applications. Mapping the stator inductance is more accessible by offline testing and then stored as lookup tables for control purposes [88]. Still, the offline measurement of stator inductance is time-consuming and is not available for a general-purpose motor drive. In this regard, motor parameter adaptation schemes are emphasized in position observer design. A general control diagram of motor-parameter-adaptive position-sensorless control is depicted in Fig. 15.

2) ADAPTIVE FILTERS

Adaptive filters are commonly adopted in parameter estimation for robust PMSM position-sensorless control, such as recursive least square (RLS) [89]–[91], affine projection algorithm (APA) [92], and EKF [93]–[95]. First, the RLS determines the weight coefficient matrix of an adaptive parameter estimator, which minimizes the sum of squares of estimation errors between the known quantities and the estimates. In [89], combined with an EEMF model with known flux linkage, the RLS is employed to estimate the stator resistance and dq-axis inductance simultaneously of both SPMSMs and IPMSMs. Whereas the multiparameter estimation of PMSMs suffers from a rank-deficient problem, which may result in ill-convergence in estimates, especially for sensorless motor drives [96]. For single-parameter estimation (e.g., stator resistance), the RLS shows robust performance by using a predefine inductance lookup table in the estimation process, which can avoid the rank-deficient issue [90]. Another approach by increasing the observer rank is to inject additional signals into the stator [90]. Dual RLSs can identify the inverter voltage distortion and the q-axis inductance, while other parameters are assumed to be constant. Second, a multiscale framework with APAs is reported

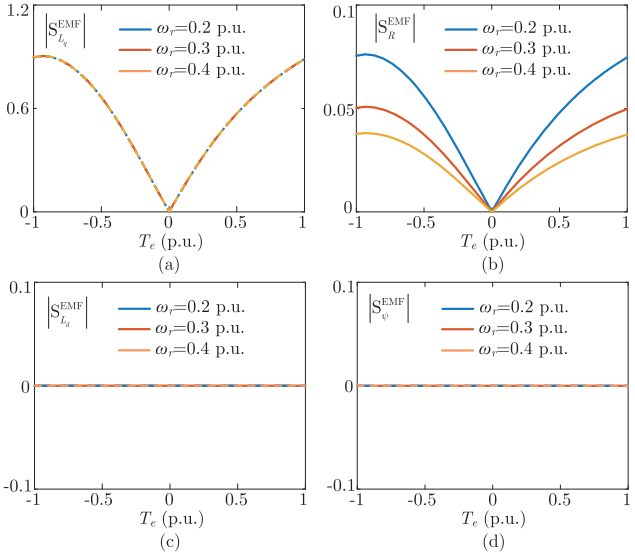

FIGURE 14. Model sensitivity analyses of EEMF-based position estimation via sensitivity functions [86] (Motor parameters are referred to [84]) (a) q-axis inductance sensitivity. (b) Stator resistance sensitivity. (c) d-axis inductance sensitivity. (c) Flux linkage sensitivity.

in [92] to estimate the stator resistance and inductance in two timescales. The stator resistance estimator is executed at a lower sampling rate since the resistance variation is slowly varying with the temperature. The inductance estimator is run at a faster sampling rate for better dynamic performance under current changes. This solution can eliminate the ill-convergence in multiparameter estimation. Still, the interaction between the two estimators and the global stability analysis needs further investigation. For the last category, the EKF is emphasized in sensorless parameter estimation due to its excellent noise suppression capability [94]. Two independent reduced-order EKFs proposed in [95] can estimate the flux linkage and stator resistance, but the two parameters cannot be estimated simultaneously. In [93], the dual-estimator concept is adopted by combining an EKF-based flux linkage estimator with a model reference adaptive system for speed/position estimation. The authors showed that the convergence and stability issues of multiparameter estimation can be solved. To sum up, the motor parameters can be well identified by the adaptive filtering algorithm with good accuracy. However, the main concern of such techniques is the high computational burden due to the matrix manipulation.

3) STATE OBSERVERS

In sensorless parameter estimation, state observers are also gained broad attention due to the simpler implementation. The commonly adopted state observers are MRAS [97]–[99], SMO [45], [47], [100], [101], and LDO [15], [59], [61], [96].

First, the MRAS utilizes the mathematical model of the PMSM with estimated parameters to compare the real system. The difference between the measured quantities, such as state currents, and the reference model outputs, converges the parameter estimation. In [97], the MRAS is used to estimate

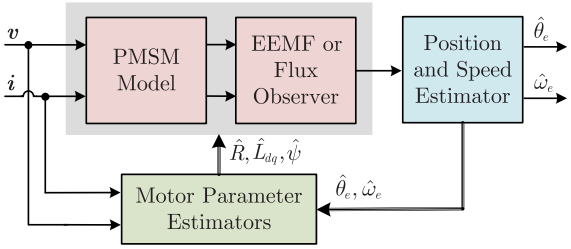

FIGURE 15. The control diagram of motor-parameter-adaptive position observers.

the stator resistance in sensorless control by adopting the γ-axis (i.e., estimated q-axis) current equation as the reference model. In [98], three MRAS estimators are designed to estimate the rotor speed/position, stator resistance, and flux linkage. The results show that estimating the three variables at the same time is impossible in this method, and only the stator resistance can be updated online for stable sensorless control. In [99], a modified MRAS with first-order low-pass filters for stator resistance and flux linkage is used in a stator feedforward voltage estimation-based sensorless control system. A stable estimation is achieved under full load from a low speed to a nominal speed.

Second, the SMO shows excellent convergence performance and stability in parameter estimation of sensorless PMSM drives. In [45], a sigmoid function-based SMO estimates the stator resistance and EEMF with reduced chattering in SPMSM position-sensorless control. The stability of position and resistance estimators can be guaranteed by adequately selecting the control gains based on the Lyapunov stability theorem. To improve the dynamic performance, the SMO proposed in [45] is upgraded to an iterative controller that executes the SMO multiple times within one control cycle [101]. Further, a STO-based SMO is reported in [47] to eliminate the chattering problem in position estimation. The stator resistance estimation is then implemented by a conventional SMO structure to update the parameter in the STA-SMO. Besides estimating one parameter, the SMO is also adopted for multiple parameter estimation in a stator flux-based position estimator [100]. In this method, the stator resistance estimator and the inductance estimator only update one parameter and treat another as a constant. For most SMO-based schemes, the main limitation is the chattering problem, while some chattering-free SMO approaches aggravate the computational burden due to the complicated structure.

Another solution for adaptive parameter estimation in sensorless control is the LDO. Same as the SMO, the LDO utilizes the error information between the measurement and the estimator output to correct the estimated parameter. The variable-structure controller in SMOs is replaced by the linear controller, such as proportional controllers, to avoid chattering issues. As a cost, the convergence rate is slower compared to the SMO. In [59], the temperature-related parameters, including the stator resistance and flux linkage, are estimated at low speed and high speed, respectively, by the LDO. The separate design in estimation can avoid the rank-deficient problem. In [61], the stator

resistance estimator is embedded in a stator flux-based speed estimator for wide-speed parameter estimation, and the robust gain selection is achieved by considering the local stability of the closed-loop estimation system. A q-axis inductance identification method is analyzed in [15] using an adaptive PI controller with the assistance of high-frequency sinusoidal current injection, but other motor parameters are not estimated. Furthermore, a comprehensive multiple parameter estimation scheme in sensorless control is designed in [96]. Unlike the previous methods that cannot estimate all parameters, the adopted approach can estimate the stator resistance, stator inductance, and flux linkage of a sensorless SPMSM drive simultaneously. The rank-deficiency and ill-convergence can be solved by injecting high-frequency signals into the stator.

4) OTHER APPROACHES

Other parameter-adaptive sensorless control methods treat the parameter estimation problem in new directions [102]–[104]. As mentioned before, the simultaneous estimation of the stator resistance and flux linkage in steady-state is rank-deficient. The solution proposed in [102] solves this issue by considering the odd-harmonic EEMF in the PMSM drive. Besides the fundamental components used in conventional methods, the fifth and seventh harmonic EEMFs in the PMSM provide additional information. The system rank can increase by two, and the multiple estimations of stator resistance and flux linkage can then be realized. Still, the universality of the method needs further investigation since the harmonic EEMFs are related to machine design and the inverter nonlinearity. In [103], a numerical method is proposed to estimate the multiple parameters in the motor starting stage. Currents and voltages are stored in a limited time series, and a polynomial method is used to calculate the motor parameters (including the rotor position) from the stored time-series data. As a possible limitation, the adopted method in [103] is only used for initial parameter determination, while the online estimation performance in rotating conditions is not validated. In [104], a straightforward parameter estimation method is proposed, in which the stator inductance is estimated by calculating the induced current magnitude under high-frequency voltage injection. The stator resistance is calculated by injecting a dc voltage into the α-axis. Compared to previous methods, no adaptation laws and stabilization are required, and the parameter estimation is independent of the position estimator. However, more extra excitation voltages are injected into the machine, which may cause larger torque ripples and power losses.

A summarized table of some critical features is given in Table 3 to compare the existing motor-parameter-adaptive position observers.

C. FREQUENCY-ADAPTIVE POSITION OBSERVERS

Frequency-adaptive position observers have drawn increasing attention recently in high-speed PMSM sensorless control due to the higher estimation accuracy under distorted conditions. Most of the existing position observers exhibit a low-pass frequency characteristic, such as SMO [25], [41], [45], [105], [106], PLL-based open-loop estimation [76], [84], [107], and disturbance observers [108]–[112]. These observers can reduce the current measurement noises due to the low-pass frequency response or improve the load transient performance based on the disturbance compensation. However, PMSM drives often contain other distortions from current measurement, inverters, and modulations, resulting in periodic position estimation errors in sensorless control [113].

1) SOURCES OF DISTORTIONS

One of the distortions in position estimation is the dc offset [113]–[117]. Current measurement bias often exists in industrial motor drives due to the inaccurate current sensor calibration or temperature increment. Through the current regulators, the current bias can lead to offsets in the reference voltages. As reported in [52], the inverter nonlinearity can also cause voltage offsets due to the bias current, as illustrated in Fig. 16. As a consequence, these offset disturbances degrade the performance of either the flux estimation or EEMF estimation-based methods. It has a more adverse effect in the flux estimation since the pure integration calculation leads to infinite flux estimation [114]. The dc offset in the stationary-frame estimated flux or EEMF can further introduce electrical-frequency fluctuating errors in the rotor position estimation [113]. The disturbance in the estimated EEMF $\hat{\boldsymbol{e}}$ (as an example) and the position estimation error are expressed as:

$$\begin{cases} \hat{\boldsymbol{e}} = \boldsymbol{e} + \boldsymbol{d}_{dc} \\ \tilde{\theta}_e = M_{dc} \sin(\omega_e t + \varphi_{dc}) \end{cases} \tag{13}$$

where $\boldsymbol{d}_{dc}$ is the dc distortion, and M_{dc} and φ_{dc} are the magnitude and phase of the position error caused by the dc offset, respectively.

Inverter nonlinearity not only increases the voltage offset under zero-current conditions, but also is a primary source of odd-order harmonics in flux and EEMF estimation [118]. The inverter nonlinearity in PMSM motor drives is caused by parasitic parameters of semiconductor devices and pulse-width modulation (PWM) deadtime [119]. It leads to voltage distortion between the reference voltage and the output voltage, which is an approximate sign function of the phase current, as illustrated previously in Fig. 16. By adopting the Fourier series on the inverter nonlinearity characteristic, the phase voltage distortion can be decomposed into odd-order harmonics, of which negative fifth and positive seventh distortions are dominant [118]. The tripled harmonics can be canceled out and thus do not exist in the three-phase Y-connected motor. Some research reports that the flux spatial harmonics could also result in the same odd-order distortions in the EEMF [120]. These odd harmonic interferences cause torque ripples in PMSM drives and also generate sixth position estimation errors, as expressed in (14).

TABLE 3. Summary and comparison of the motor-parameter-adaptive position observers for sensorless PMSM drives.

Motor-Parameter-Adaptive Position Observers	Parameter Estimation Methods	Convergence Rate	Robustness to Noises	Computational Complexity	Advantages	Disadvantages
Adaptive Filters	RLS [89]–[91]	Fast	Medium	High	Good convergence performance and estimation accuracy	High computational burden, ill-convergence in multiparameter estimation
	APA [92]	Medium	Medium	Medium	Multiparameter estimation	Complex stepsize selection
	EKF [93]–[95]	Medium	High	High	Anti-measurement-noise capability	Computational burden
State Observers	MRAS [97]–[99]	Medium	Medium	Medium	Multiparameter estimation, wide operation range	Time-consuming gain tunings
	SMO [45], [47] [100], [101]	Fast	Medium	High	Fast convergence and robustness	Chattering problem, high computational burden in advanced SMOs
	LDO [59], [61] [15], [96]	Medium	Medium	Low	Simple structure, low computational burden	Lower dynamic performance
Other Approaches	Harmonic EMF [102]	Medium	Medium	Medium	Multiparameter estimation without additional injection	Low universality
	Numerical method [103]	Fast	Low	Medium	No tunable parameters	Offline method, high sensitivity to noises
	Signal injection [104]	Fast	High	Low	Simple implementation	Voltage and current distortions by high-frequency and dc injection

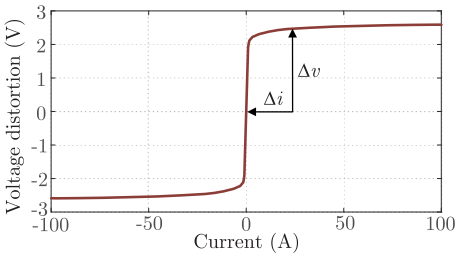

FIGURE 16. Voltage distortion caused by inverter nonlinearity.

A straightforward solution to compensate for the impact is using voltage feedforward based on a predefine inverter nonlinearity lookup table. However, it requires time-consuming offline measurement, and the digital delay would limit the compensation accuracy at high speed [121].

$$\begin{cases} \hat{\boldsymbol{e}} = \boldsymbol{e} + \boldsymbol{d}_{-5th} + \boldsymbol{d}_{7th} \\ \tilde{\theta}_e = M_{6th} \sin(6\omega_e t + \varphi_{6th}) \end{cases} \tag{14}$$

where $\boldsymbol{d}_{-5th}$ and $\boldsymbol{d}_{7th}$ are the dominant odd-order harmonics, and M_{6th} and φ_{6th} are the magnitude and phase of the sixth position error.

Unlike the broadly concerned dc offset and odd-order harmonic effects on PMSM position estimation, even-order harmonics are rarely analyzed. This distortion is generated by the space-vector PWM (SVPWM) [122], in which the line-to-line voltage of the inverter is not half-wave symmetrical. Thus, the modulated voltage fed to the PMSM would contain even-order harmonics, among them the second and fourth components are dominant, as expressed in (15). The even-order disturbance has little influence at a high carrier-to-fundamental frequency ratio, namely at lower speed with a higher switching frequency. Still, it should be considered in ultra-high-speed cases since the harmonics from the SVPWM cannot be neglected.

$$\begin{cases} \hat{\boldsymbol{e}} = \boldsymbol{e} + \boldsymbol{d}_{-2th} + \boldsymbol{d}_{4th} \\ \tilde{\theta}_e = M_{3th} \sin(3\omega_e t + \varphi_{3th}) \end{cases} \tag{15}$$

where $\boldsymbol{d}_{-2th}$ and $\boldsymbol{d}_{4th}$ are the dominant even-order harmonics, and M_{3th} and φ_{3th} are the magnitude and phase of the third position error.

It can be observed that the primary distortions (13)-(15) in the estimation exhibit specific frequency characteristics, including dc offset (zero-frequency), odd-order harmonics, and even-order harmonics. Therefore, frequency-adaptive position observers would be effective solutions to address the problem.

2) ADAPTIVE BANDPASS POSITION OBSERVERS

Adaptive bandpass position observers [19], [37], [81], [113]–[115], [123]–[127] are better candidates in dealing with the dc-offset issue compared to conventional low-pass position observers. The adaptive observers are often upgraded from advanced PLL techniques used in grid-connected converters [128]–[133]. A general control diagram of the adaptive bandpass position observer is given in Fig. 17. The stator flux or EEMF is first estimated from a conventional low-pass estimator (e.g., SMO) but contains nonideal distortions. An adaptive bandpass filter is then employed as an in-loop controller to suppress the disturbances. Last, the PLL is

TABLE 4. Summary and comparison of the frequency-adaptive position observers for sensorless PMSM drives.

Frequency-Adaptive Position Observers	Techniques	dc-Offset	Low-Order Harmonics	Computational Burden	Advantages	Disadvantages
Adaptive Bandpass Position Observers	Second-order bandpass filter [37]	Reduced	Reduced	Medium	Simple structure and implementation	Weak dc-offset suppression, additional phase compensation
	SOGI/Quasi-SOGI [19], [123]–[126]	Eliminated	Reduced	Medium	dc-offset elimination capability	Only available for a single input signal
	High-order SOGI [114], [115]	Eliminated	Reduced	High	dc-offset elimination of both the input signal and its quadrature form	High computational burden
	PR controller [81], [127]	Reduced	Reduced	Medium	Embeddable controller in state-feedback systems	Limited dc-offset suppression
	CC observer [113]	Reduced	Reduced	Low	Robustness and low computational burden	Limited dc-offset suppression
Adaptive MHE Position Observers	Multiple adaptive bandpass observer [118], [135]	Eliminated	Eliminated odd harmonics	High	Multiple harmonic elimination, cascaded structure	High computational burden, complicated parameter design
	Learning mechanism [134], [136]–[138]	Not suppressed	Eliminated odd harmonics	High	Fast convergence	High computational burden
	Comb observer [139]	Eliminated	Eliminated odd and even harmonics	Low	Elimination of all primary distortions, robustness, low computational burden	Additional memory space
	Iterative learning control [140]	Eliminated	Eliminated odd and even harmonics	Medium	Elimination of all primary distortions	Parameter tuning related to rotor speed

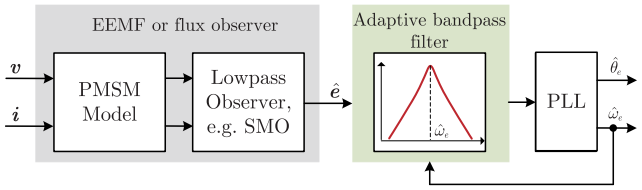

FIGURE 17. General control diagram of adaptive bandpass position observers [123].

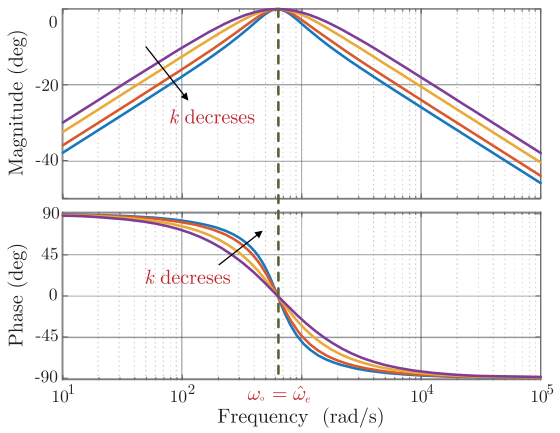

FIGURE 18. Bode diagram of the SOGI.

adopted to estimate the rotor speed and position from the filtered flux or EEMF estimation.

A typical adaptive bandpass position observer is based on the second-order generalized integrator (SOGI) and can be used for flux estimation-based sensorless control [123]. The Bode diagram and transfer function are given in Fig. 18 and (16), respectively. The SOGI possesses unity-magnitude and zero-phase characteristics around the central frequency ω_o, while offering decayed magnitude at low and high frequencies. Therefore, by selecting the central frequency equal to the estimated rotor frequency $\hat{\omega}_e$, the SOGI-based estimator can extract the fundamental flux or EEMF while suppressing the dc offset and noise interferences. The estimated position from the fundamental flux or EEMF also has no phase lag due to the zero-phase property at the fundamental frequency. Besides applying a standard SOGI, recent research upgrades the SOGI to the third-order and fourth-order position observers to further enhance the dc-offset filtering capability of both the input signal and its quadrature form [114], [115].

$$G = \frac{k\omega_o s}{s^2 + k\omega_o s + \omega_o^2} = \frac{k\hat{\omega}_e s}{s^2 + k\hat{\omega}_e s + \hat{\omega}_e^2} \tag{16}$$

Similar to the SOGI, the adaptive bandpass observer can be established on other structures. In [37], the bandpass EEMF estimation is realized by combining a first-order high-pass filter and a low-pass filter. Different from the SOGI that introduces zero phase error, the method needs a speed-related compensation unit to correct phase delay caused by

first-order filters. In [19], [124]–[126], quasi-SOGI adaptive observers are employed as the in-loop filters for dc-offset reduction. These observers have slightly different transfer functions from the SOGI and can achieve the same filtering capability in eliminating the dc offset. Another widely concerned approach used as the adaptive bandpass position observer is the proportional-resonant (PR) controllers. The PR controller replaces the linear and variable-structure controllers in the flux or EEMF observers. All estimates in the observers, including the flux, EEMF and current estimation, can exhibit robust noise-suppression capability. For instance, Bao *et al.* explored the PR controller to address the chattering problem in the sliding-mode EEMF estimator and reduce the harmonic content in the estimated current and EEMF [127]. The work presented in [81] improves the performance of the PR-based observer under low carrier ratio.

Although the adaptive bandpass position observers achieve enhanced robustness against dc distortion than conventional schemes, there are still critical concerns in the system nonlinearity and stability. In most methods, speed/frequency adaptation is realized by feedbacking the estimated speed of the PLL, but it results in highly nonlinear control structure. Observer stability becomes ambiguous and hard to be guaranteed in such a nonlinear system. The issue does not trouble the original application of adaptive filters in the grid-connected converter since the grid frequency fluctuates very slightly [130]. However, the rapid varying rotor frequency of high-speed PMSMs poses a challenge in the adaptive observer design, but the issue is ignored in most literature. Although the SOGI adopts a frequency-locked loop and does not use the feedback estimated speed, the observer parameters need careful tuning for stability. Recently. a research work proposed in [113] analyzes the stability issue of a complex-coefficient (CC) adaptive bandpass observer and gives a parameter design scheme. A speed adaptation law is obtained based on the Lyapunov stability theorem, and small-signal approximation is used to linearize the nonlinear observer to facilitate the parameter tuning. As a cost, the dc offset cannot be entirely removed compared to the SOGI-based observer.

3) ADAPTIVE MULTIPLE-HARMONIC-ELIMINATION (MHE) POSITION OBSERVERS

The aforementioned adaptive bandpass position observers are superior in dc offset suppression, but the capability in low-order harmonic elimination is not enhanced. Low-order distortions, such as second/fourth harmonics generated from the SVPWM and the fifth/seventh harmonics caused by the inverter nonlinearity, are non-negligible and need to be addressed in position estimation. For the adaptive bandpass position observers, the decaying magnitude frequency characteristic in the high-frequency region can provide some low-order harmonic reduction ability, as illustrated in Fig. 18. Still, the performance is usually not satisfactory. Deceasing the observer bandwidth is a solution to facilitate better harmonic rejection in the steady-state, but it would lead to transient estimation errors and even instability.

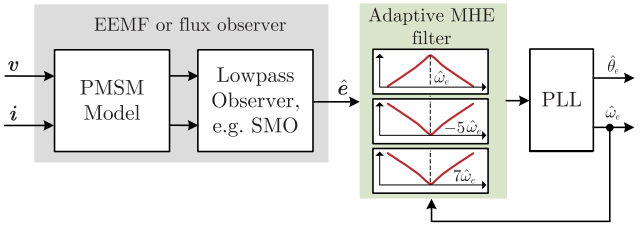

FIGURE 19. A general control diagram of adaptive MHE position observers [118].

Adaptive MHE position observers are therefore proposed to eliminate the low-order harmonics [118], [134]–[140]. A representative structure is given in Fig. 19. Compared to the bandpass observer that utilizes a single in-loop bandpass filter in flux or EEMF estimation, the MHE observers contain a bandpass filter that extracts the fundamental component and several bandstop filters to cancel the selected-frequency low-order harmonics. The bandstop filter often has the same structure as the bandpass filter but with an inverse magnitude characteristic.

Wang *et al.* proposed an adaptive MHE position observer by employing several SOGIs in parallel to eliminate the fifth and seventh EEMF harmonics [118]. It is an upgrade from the SOGI-based bandpass observer by adding two SOGI-based bandstop filters with the notching frequencies at $5\hat{\omega}_e$ and $7\hat{\omega}_e$, respectively. The transfer function the MHE structure is expressed in (17), and the Bode diagram is shown in Fig. 20. As observed, two notching points at the selected harmonic frequencies are generated with zero-magnitude response, thereby eliminating the selected low-order harmonics. Since the SOGI frequency characteristics are symmetric in both positive and negative frequency ranges, the design of notching feature at $5\hat{\omega}_e$ and $7\hat{\omega}_e$ also works at $-5\hat{\omega}_e$ and $-7\hat{\omega}_e$. Therefore, the primary distortion of $-5\hat{\omega}_e$ and $7\hat{\omega}_e$ harmonics caused by inverter nonlinearity can be eliminated by the SOGI-based observer. However, for some bandpass filters, the frequency characteristic is asymmetric, and thus the notching design should consider the sign of the harmonic. Besides the SOGI, other types of adaptive bandpass filters can be employed in series or parallel to configure the MHE position observer, such as the vector filter proposed in [135].

$$G_{MHE} = G_1 \frac{1 - G_5 - G_7 + G_5 G_7}{1 - G_5 G_7 - G_1 G_5 - G_1 G_7 + 2 G_1 G_5 G_7} \tag{17}$$

where G_1, G_5, G_7 are the transfer functions of the SOGI with the central frequency of ω_e, $5\omega_e$, and $7\omega_e$, respectively.

Another class of adaptive MHE position observers is the learning mechanism method. By monitoring the operating conditions of the PMSM, learning units or networks in the observer can self-adjust weighting factors and adapt the harmonic characteristic in position estimation. The structure of the learning mechanism-based MHE observer is shown in Fig. 21. The learning mechanism is often selected as the RLS algorithm or the least-mean-square (LMS) algorithm.

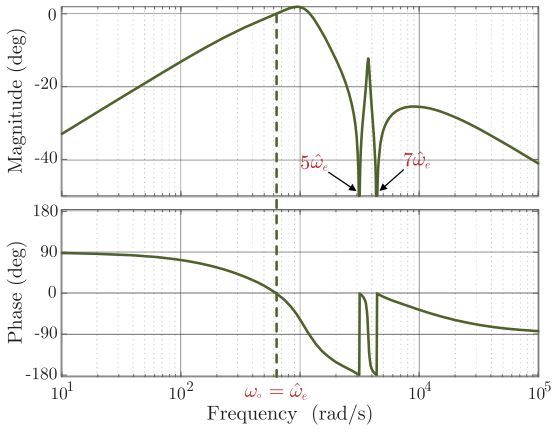

FIGURE 20. Bode diagram of the MHE-SOGI.

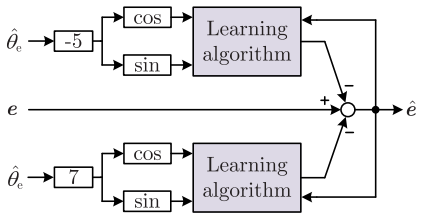

FIGURE 21. Structure of the learning mechanism-based MHE observer [138].

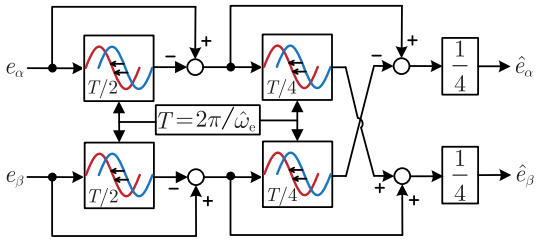

FIGURE 22. Structure of the MHE adaptive comb filter [139].

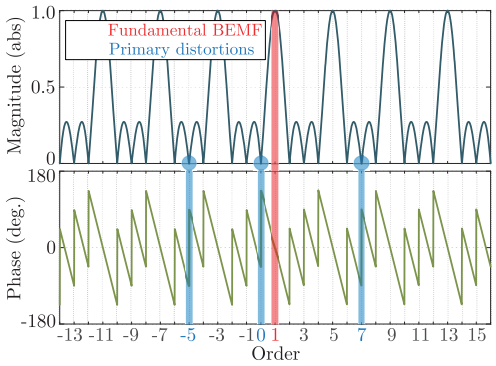

FIGURE 23. Bode diagram of the MHE adaptive comb filter [139].

In [136], the RLS algorithm combined with a sliding-mode EEMF estimator is proposed to filter the fifth and seventh harmonics adaptively. Filter coefficients and gains can be updated online through autocorrelation matrixes. In [137], an LMS algorithm is adopted with fifth and seventh harmonic estimation branches for adaptive MHE in position estimation. Comparative studies of the RLS-based and LMS-based adaptive filtering network are conducted in [134], which validates that the RLS algorithm has better dynamic performance with lower ripples in position and speed estimation. An enhanced learning mechanism using a bilinear RLS adaptive filter is analyzed in [138], which can enhance the convergence rate and motor stiffness further.

Though more harmonic components are considered in the adaptive MHE position observers than bandpass techniques, the increasing computational burden due to the complicated filtering network limits the potential application in industrial PMSM drives [139]. Besides, the high-order system requires more accurate discretization methods, especially at high speed [141], which makes the digital implementation complicated. To ease the problem, a recent work proposed in [139] adopts an adaptive comb filter for MHE position estimation. The adaptive comb filter is developed from the moving average filter used in grid-connected control [132] but with improved dynamic performance contributed by a Lyapunov-theorem-based frequency-locked loop. This approach does not use the high-order filtering network; instead, a more straightforward structure shown in Fig. 22 can provide notching characteristics for primarily odd-order and even-order distortions according to the Bode diagram in Fig. 23. Besides, the observer is configured by several digital delay operators, which results in an easier discrete implementation than the high-order filtering network. Another approach with reduced computational burden proposed in [140] utilizes the iterative learning control for adaptive voltage compensation. The method can consider all possible distortions as a unified disturbance, and a single iterative learning algorithm can converge the unified perturbance to zero by generating a feedforward compensation voltage.

Similar to the adaptive bandpass position observer, most of the existing MHE research does not analyze the stability and parameter design scheme due to the complicated observer structure [118], [134]–[138]. A recent attempt is to linearize the MHE position observer around its fundamental frequency [139], in which the bandwidth and phase margin can be approximated obtained. A proposed speed adaptation law can locally guarantee observer stability, and a parameter design scheme is given according to the linearized model. However, modeling errors are inevitable due to the approximation in the position observer and cause some theoretical mismatch, and thus more investigations are needed.

A summary and comparison table of the frequency-adaptive position observers is given in Table 4.

IV. FUTURE WORK

While the sensorless PMSM control techniques have been studied from decades ago to now, improvements can still be performed in the existing algorithms. This section examines the future trends in this topic.

A. OBSERVER ROBUSTNESS EXPANSION FOR HIGH SPEED SENSORLESS CONTROL UNDER LOW SAMPLING FREQUENCY

From the new PMSM sensorless research topics presented in section III, the operation under low f_{ratio} has the fewest studies. The current design algorithms still lack of robustness analysis tools and, since the FOO is shown to have its stability dependent on the actual rotor speed, the discrete-time observer design should evaluate the robustness in relation to speed estimation error. Thus, it will be possible to evaluate and extract the lowest f_{ratio} for each operation point. The analysis of the effects of the sampling frequency on the rotor position and speed estimation, similarly to the parameter variation analysis already presented in the literature, should also be performed. Furthermore, design procedures robust to parameter variation can also expand the f_{ratio} that proved to be limited when the PMSM is under load.

B. IMPROVEMENT IN PARAMETER ESTIMATION FOR PMSM SENSORLESS CONTROL

Motor parameter estimation in position-sensorless control of PMSMs still has challenges in the full-speed region. First, existing approaches are almost model-based, which are unavailable at zero speed due to the low signal-to-noise ratio. Hence, parameter estimation may suffer from low accuracy or be unstable under standstill conditions. Second, the rank-deficiency in multiparameter estimation is often solved by injecting additional signals into the stator. Still, it limits the machine' output power and cannot be used for a high-speed motor drive. Consequently, a full-speed parameter estimation scheme is expected. In addition, the parameter estimation of the IPMSM is more complicated than the SPMSM due to the decoupling between the dq-axes and more parameters (i.e., two inductances), while most of the work studies on the SPMSM. Advanced parameter estimation strategies could be investigated for IPMSM drives.

C. PERFORMANCE ENHANCEMENT IN FREQUENCY-ADAPTIVE POSITION OBSERVERS

First, the low-speed performance of the frequency-adaptive position observers needs to be improved. These observers are usually adopted in model-based position-sensorless control at high speed because the frequency difference between the fundamental component and harmonics is significant, making the fundamental signal extraction and harmonic elimination easier. However, the frequency difference becomes indistinguishable at zero and low speed. A reduced bandwidth is often required at a lower speed for to maintain accurate position estimation without harmonics. Still, the dynamic performance would be degraded and even cannot support the stable driving. More attention can be drawn in the future to enhance the distortion rejection capability for low-speed operation.

Second, the dynamic performance of the position observer should be further improved. The frequency-adaptive observers inevitably introduce transient phase delay in position estimation. It causes transient position estimation errors when the rotor speed changes rapidly. Due to the nonlinear observer structure, it is necessary to research on observer linearization to analyze the stability property and dynamic characteristics. An instructive parameter design scheme needs to be given to for adequate trade-off between the dynamic performance and harmonic rejection capability. Moreover, the high-bandwidth adaptive position observer design would be another interesting direction to enhance the dynamic performance.

Another possible research direction is to combine the motor parameter estimation with the frequency-adaptive position observers. The existing frequency-adaptive observer designs are all model-based, while the motor parameter mismatch would cause additional position estimation errors. Hence, cooperating with an online parameter identification method will be an attractive research work to enhance the sensorless control performance. However, it raises a challenge that the nonideal distortions in PMSM drives can also lead to inaccurate motor parameter estimation. The frequency-adaptive mechanism needs to be adopted in the parameter estimation scheme to improve the identification accuracy. In terms of complexity and computational burden, using a single frequency-adaptive observer to estimate the rotor position and motor parameters simultaneously will be more industry-oriented. For this nonlinear estimator, the stability and optimal parameter design are crucial issues.

V. CONCLUSION

The PMSM sensorless methods have been widely used due to its cost and volume reduction capabilities, which leads to a vast research in order to achieve similar performance from the drives with sensor. A comprehensive review of observer methods for position sensorless PMSM drives, as well with the major tuning challenges for high performance estimation under non-ideal driven conditions, is presented in this paper. First, the major observer algorithms, used to improve the estimation performance from the standard open-loop method, with its design and stability constraints are investigated. Then, the dominant recent research topics are presented, which are the maintenance of estimation performance under low-sampling frequency and parameter estimation for position sensorless enhancement. Frequency-adaptive observers for harmonic reduction and performance improvement is also investigated.

REFERENCES

[1] M. Pacas, "Sensorless drives in industrial applications," *IEEE Ind. Electron. Mag.*, vol. 5, no. 2, pp. 16–23, Jun. 2011.

[2] G.-A. Capolino and A. Cavagnino, "New trends in electrical machines technology—Part II," *IEEE Trans. Ind. Electron.*, vol. 61, no. 9, pp. 4931–4936, Sep. 2014.

[3] G. Wang, M. Valla, and J. Solsona, "Position sensorless permanent magnet synchronous machine drives—A review," *IEEE Trans. Ind. Electron.*, vol. 67, no. 7, pp. 5830–5842, Jul. 2020.

[4] A. B. Plunkett and F. G. Turnbull, "Load-commutated inverter/synchronous motor drive without a shaft position sensor," *IEEE Trans. Ind. Appl.*, vol. IA-15, no. 1, pp. 63–71, Jan. 1979.

[5] K. Iizuka, H. Uzuhashi, M. Kano, T. Endo, and K. Mohri, "Microcomputer control for sensorless brushless motor," *IEEE Trans. Ind. Appl.*, vol. IA-21, no. 3, pp. 595–601, May 1985.
[6] J. Davoine, R. Perret, and H. Le-Huy, "Operation of a self-controlled synchronous motor without a shaft position sensor," *IEEE Trans. Ind. Appl.*, vol. IA-19, no. 2, pp. 217–222, Mar. 1983.
[7] R. Wu and G. R. Slemon, "A permanent magnet motor drive without a shaft sensor," *IEEE Trans. Ind. Appl.*, vol. 27, no. 5, pp. 1005–1011, Sep. 1991.
[8] R. B. Sepe and J. H. Lang, "Real-time observer-based (adaptive) control of a permanent-magnet synchronous motor without mechanical sensors," *IEEE Trans. Ind. Appl.*, vol. 28, no. 6, pp. 1345–1352, Nov. 1992.
[9] M.-H. Park and H.-H. Lee, "Sensorless vector control of permanent magnet synchronous motor using adaptive identification," in *Proc. 15th Annu. Conf. IEEE Ind. Electron. Soc.*, Nov. 1989, pp. 209–214.
[10] A. Consoli, S. Musumeci, A. Raciti, and A. Testa, "Sensorless vector and speed control of brushless motor drives," *IEEE Trans. Ind. Electron.*, vol. 41, no. 1, pp. 91–96, Feb. 1994.
[11] M. Tomita, T. Senjyu, S. Doki, and S. Okuma, "New sensorless control for brushless DC motors using disturbance observers and adaptive velocity estimations," *IEEE Trans. Ind. Electron.*, vol. 45, no. 2, pp. 274–282, Apr. 1998.
[12] N. Matsui, "Sensorless PM brushless DC motor drives," *IEEE Trans. Ind. Electron.*, vol. 43, no. 2, pp. 300–308, Apr. 1996.
[13] T.-H. Liu and C.-P. Cheng, "Adaptive control for a sensorless permanent-magnet synchronous motor drive," *IEEE Trans. Aerosp. Electron. Syst.*, vol. 30, no. 3, pp. 900–909, Jul. 1994.
[14] R. Krishnan, *Permanent Magnet Synchronous and Brushless DC Motor Drives*. Boca Raton, FL, USA: CRC Press, 2009.
[15] M. Hasegawa and K. Matsui, "Position sensorless control for interior permanent magnet synchronous motor using adaptive flux observer with inductance identification," *IET Electr. Power Appl.*, vol. 3, no. 3, pp. 209–217, May 2009.
[16] Z. Chen, M. Tomita, S. Doki, and S. Okuma, "An extended electromotive force model for sensorless control of interior permanent-magnet synchronous motors," *IEEE Trans. Ind. Electron.*, vol. 50, no. 2, pp. 288–295, Apr. 2003.
[17] I. Boldea, M. C. Paicu, and G.-D. Andreescu, "Active flux concept for motion-sensorless unified AC drives," *IEEE Trans. Power Electron.*, vol. 23, no. 5, pp. 2612–2618, Sep. 2008.
[18] Y. Zhao, Z. Zhang, W. Qiao, and L. Wu, "An extended flux model-based rotor position estimator for sensorless control of salient-pole permanent-magnet synchronous machines," *IEEE Trans. Power Electron.*, vol. 30, no. 8, pp. 4412–4422, Aug. 2015.
[19] X. Song, J. Fang, B. Han, and S. Zheng, "Adaptive compensation method for high-speed surface PMSM sensorless drives of EMF-based position estimation error," *IEEE Trans. Power Electron.*, vol. 31, no. 2, pp. 1438–1449, Feb. 2016.
[20] S. Sangwongwanich, S. Suwankawin, S. Po-Ngam, and S. Koonlaboon, "A unified speed estimation design framework for sensorless AC motor drives based on positive-real property," in *Proc. Power Convers. Conf. (Nagoya)*, Apr. 2007, pp. 1111–1118.
[21] P. Vaclavek, P. Blaha, and I. Herman, "AC drive observability analysis," *IEEE Trans. Ind. Electron.*, vol. 60, no. 8, pp. 3047–3059, Aug. 2013.
[22] M. Koteich, A. Maloum, G. Duc, and G. Sandou, "Discussion on 'ac drive observability analysis,'" *IEEE Trans. Ind. Electron.*, vol. 62, no. 11, pp. 7224–7225, Jun. 2015.
[23] D. Zaltni, M. N. Abdelkrim, M. Ghanes, and J. P. Barbot, "Observability analysis of PMSM," in *Proc. 3rd Int. Conf. Signals, Circuits Syst. (SCS)*, Nov. 2009, pp. 1–6.
[24] J. Zhao, S. Nalakath, and A. Emadi, "A high frequency injection technique with modified current reconstruction for low-speed sensorless control of IPMSMs with a single DC-link current sensor," *IEEE Access*, vol. 7, pp. 136137–136147, 2019.
[25] G. Foo and M. F. Rahman, "Sensorless sliding-mode MTPA control of an IPM synchronous motor drive using a sliding-mode observer and HF signal injection," *IEEE Trans. Ind. Electron.*, vol. 57, no. 4, pp. 1270–1278, Apr. 2010.
[26] G.-D. Andreescu, C. I. Pitic, F. Blaabjerg, and I. Boldea, "Combined flux observer with signal injection enhancement for wide speed range sensorless direct torque control of IPMSM drives," *IEEE Trans. Energy Convers.*, vol. 23, no. 2, pp. 393–402, Jun. 2008.
[27] J.-H. Jang, J.-I. Ha, M. Ohto, K. Ide, and S.-K. Sul, "Analysis of permanent-magnet machine for sensorless control based on high-frequency signal injection," *IEEE Trans. Ind. Appl.*, vol. 40, no. 6, pp. 1595–1604, Nov. 2004.
[28] S. Kim, J.-I. Ha, and S.-K. Sul, "PWM switching frequency signal injection sensorless method in IPMSM," *IEEE Trans. Ind. Appl.*, vol. 48, no. 5, pp. 1576–1587, Sep. 2012.
[29] J. M. Liu and Z. Q. Zhu, "Novel sensorless control strategy with injection of high-frequency pulsating carrier signal into stationary reference frame," *IEEE Trans. Ind. Appl.*, vol. 50, no. 4, pp. 2574–2583, Jul. 2014.
[30] S.-C. Yang, "Saliency-based position estimation of permanent-magnet synchronous machines using square-wave voltage injection with a single current sensor," *IEEE Trans. Ind. Appl.*, vol. 51, no. 2, pp. 1561–1571, Mar. 2015.
[31] J.-H. Im and R.-Y. Kim, "Improved saliency-based position sensorless control of interior permanent-magnet synchronous machines with single DC-link current sensor using current prediction method," *IEEE Trans. Ind. Electron.*, vol. 65, no. 7, pp. 5335–5343, Jul. 2018.
[32] J.-H. Jang, S.-K. Sul, J.-I. Ha, K. Ide, and M. Sawamura, "Sensorless drive of surface-mounted permanent-magnet motor by high-frequency signal injection based on magnetic saliency," *IEEE Trans. Ind. Appl.*, vol. 39, no. 4, pp. 1031–1039, Jul. 2003.
[33] M. Darouach, M. Zasadzinski, and S. J. Xu, "Full-order observers for linear systems with unknown inputs," *IEEE Trans. Autom. Control*, vol. 39, no. 3, pp. 606–609, Mar. 1994.
[34] W.-H. Chen, J. Yang, L. Guo, and S. Li, "Disturbance-observer-based control and related methods—An overview," *IEEE Trans. Ind. Electron.*, vol. 63, no. 2, pp. 1083–1095, Feb. 2016.
[35] C. L. Baratieri and H. Pinheiro, "Sensorless vector control for PM brushless motors with nonsinusoidal back-EMF," in *Proc. Int. Conf. Electr. Mach. (ICEM)*, Sep. 2014, pp. 915–921.
[36] L. Xiaoquan, L. Heyun, and H. Junlin, "Load disturbance observer-based control method for sensorless PMSM drive," *IET Electr. Power Appl.*, vol. 10, no. 8, pp. 735–743, Sep. 2016.
[37] W. Zhao, S. Jiao, Q. Chen, D. Xu, and J. Ji, "Sensorless control of a linear permanent-magnet motor based on an improved disturbance observer," *IEEE Trans. Ind. Electron.*, vol. 65, no. 12, pp. 9291–9300, Dec. 2018.
[38] L. Ding, Y. W. Li, and N. R. Zargari, "Discrete-time SMO sensorless control of current source converter-fed PMSM drives with low switching frequency," *IEEE Trans. Ind. Electron.*, vol. 68, no. 3, pp. 2120–2129, Mar. 2021.
[39] Q. An, J. Zhang, Q. An, X. Liu, A. Shamekov, and K. Bi, "Frequency-adaptive complex-coefficient filter-based enhanced sliding mode observer for sensorless control of permanent magnet synchronous motor drives," *IEEE Trans. Ind. Appl.*, vol. 56, no. 1, pp. 335–343, Jan. 2020.
[40] S. Chi, Z. Zhang, and L. Xu, "Sliding-mode sensorless control of direct-drive PM synchronous motors for washing machine applications," *IEEE Trans. Ind. Appl.*, vol. 45, no. 2, pp. 582–590, Mar. 2009.
[41] Z. Qiao, T. Shi, Y. Wang, Y. Yan, C. Xia, and X. He, "New sliding-mode observer for position sensorless control of permanent-magnet synchronous motor," *IEEE Trans. Ind. Electron.*, vol. 60, no. 2, pp. 710–719, Feb. 2013.
[42] Y. Zhao, W. Qiao, and L. Wu, "An adaptive quasi-sliding-mode rotor position observer-based sensorless control for interior permanent magnet synchronous machines," *IEEE Trans. Power Electron.*, vol. 28, no. 12, pp. 5618–5629, Dec. 2013.
[43] Y. Zhao, W. Qiao, and L. Wu, "Dead-time effect analysis and compensation for a sliding-mode position observer-based sensorless IPMSM control system," *IEEE Trans. Ind. Appl.*, vol. 51, no. 3, pp. 2528–2535, May 2015.
[44] W. Xu, S. Qu, L. Zhao, and H. Zhang, "An improved adaptive sliding mode observer for middle- and high-speed rotor tracking," *IEEE Trans. Power Electron.*, vol. 36, no. 1, pp. 1043–1053, Jan. 2021.
[45] H. Kim, J. Son, and J. Lee, "A high-speed sliding-mode observer for the sensorless speed control of a PMSM," *IEEE Trans. Ind. Electron.*, vol. 58, no. 9, pp. 4069–4077, Sep. 2011.
[46] A. Levant, "Sliding order and sliding accuracy in sliding mode control," *Int. J. Control*, vol. 58, no. 6, pp. 1247–1263, Dec. 1993.
[47] D. Liang, J. Li, and R. Qu, "Sensorless control of permanent magnet synchronous machine based on second-order sliding-mode observer with online resistance estimation," *IEEE Trans. Ind. Appl.*, vol. 53, no. 4, pp. 3672–3682, Jul. 2017.

[48] C. L. Baratieri and H. Pinheiro, "New variable gain super-twisting sliding mode observer for sensorless vector control of nonsinusoidal back-EMF PMSM," *Control Eng. Pract.*, vol. 52, pp. 59–69, Jul. 2016.
[49] S. R and B. Singh, "Sensorless predictive control of SPMSM-driven light EV drive using modified speed adaptive super twisting sliding mode observer with MAF-PLL," *IEEE J. Emerg. Sel. Topics Ind. Electron.*, vol. 2, no. 1, pp. 42–52, Jan. 2021.
[50] D. Liang, J. Li, R. Qu, and W. Kong, "Adaptive second-order sliding-mode observer for PMSM sensorless control considering VSI nonlinearity," *IEEE Trans. Power Electron.*, vol. 33, no. 10, pp. 8994–9004, Oct. 2018.
[51] S. Wu, J. Zhang, and B. Chai, "Adaptive super-twisting sliding mode observer based robust backstepping sensorless speed control for IPMSM," *ISA Trans.*, vol. 92, pp. 155–165, Sep. 2019.
[52] S. Bolognani, S. Calligaro, and R. Petrella, "Design issues and estimation errors analysis of back-EMF-based position and speed observer for SPM synchronous motors," *IEEE J. Emerg. Sel. Topics Power Electron.*, vol. 2, no. 2, pp. 159–170, Jun. 2014.
[53] M. Hasegawa, S. Yoshioka, and K. Matsui, "Position sensorless control of interior permanent magnet synchronous motors using unknown input observer for high-speed drives," *IEEE Trans. Ind. Appl.*, vol. 45, no. 3, pp. 938–946, May 2009.
[54] M. Hasegawa and K. Matsui, "IPMSM position sensorless drives using robust adaptive observer on stationary reference frame," *IEEJ Trans. Electr. Electron. Eng.*, vol. 3, no. 1, pp. 120–127, Jan. 2008.
[55] M. Tomita, M. Hasegawa, and K. Matsui, "A design method of full-order extended electromotive force observer for sensorless control of IPMSM," in *Proc. 11th IEEE Int. Workshop Adv. Motion Control (AMC)*, Mar. 2010, pp. 206–209.
[56] Z. Novak and M. Novak, "Design of high-speed permanent magnet synchronous motor for advanced and sensorless control techniques validation," in *Proc. 18th Int. Conf. Mechatronics Mechatronika (ME)*, Dec. 2018, pp. 1–8.
[57] S. Po-Ngam and S. Sangwongwanich, "Stability and dynamic performance improvement of adaptive full-order observers for sensorless PMSM drive," *IEEE Trans. Power Electron.*, vol. 27, no. 2, pp. 588–600, Feb. 2012.
[58] C. J. V. Filho and R. P. Vieira, "Adaptive full-order observer analysis and design for sensorless interior permanent magnet synchronous motors drives," *IEEE Trans. Ind. Electron.*, early access, Jul. 10, 2020, doi: 10.1109/TIE.2020.3007101.
[59] A. Piippo, M. Hinkkanen, and J. Luomi, "Adaptation of motor parameters in sensorless PMSM drives," *IEEE Trans. Ind. Appl.*, vol. 45, no. 1, pp. 203–212, Jan. 2009.
[60] T. Tuovinen, M. Hinkkanen, L. Harnefors, and J. Luomi, "Comparison of a reduced-order observer and a full-order observer for sensorless synchronous motor drives," *IEEE Trans. Ind. Appl.*, vol. 48, no. 6, pp. 1959–1967, Nov. 2012.
[61] M. Hinkkanen, T. Tuovinen, L. Harnefors, and J. Luomi, "A combined position and stator-resistance observer for salient PMSM drives: Design and stability analysis," *IEEE Trans. Power Electron.*, vol. 27, no. 2, pp. 601–609, Feb. 2012.
[62] A. Piippo, M. Hinkkanen, and J. Luomi, "Analysis of an adaptive observer for sensorless control of interior permanent magnet synchronous motors," *IEEE Trans. Ind. Electron.*, vol. 55, no. 2, pp. 570–576, Jan. 2008.
[63] P. Kshirsagar, R. P. Burgos, J. Jang, A. Lidozzi, F. Wang, D. Boroyevich, and S.-K. Sul, "Implementation and sensorless vector-control design and tuning strategy for SMPM machines in fan-type applications," *IEEE Trans. Ind. Appl.*, vol. 48, no. 6, pp. 2402–2413, Nov. 2012.
[64] B. Li and L. Li, "New integration algorithms for flux estimation of AC machines," in *Proc. Int. Conf. Electr. Mach. Syst.*, Aug. 2011, pp. 1–5.
[65] S. Bolognani, L. Tubiana, and M. Zigliotto, "Extended Kalman filter tuning in sensorless PMSM drives," *IEEE Trans. Ind. Appl.*, vol. 39, no. 6, pp. 1741–1747, Nov. 2003.
[66] Z. Wang, Y. Zheng, Z. Zou, and M. Cheng, "Position sensorless control of interleaved CSI fed PMSM drive with extended Kalman filter," *IEEE Trans. Magn.*, vol. 48, no. 11, pp. 3688–3691, Nov. 2012.
[67] R. Cao, N. Jiang, and M. Lu, "Sensorless control of linear flux-switching permanent magnet motor based on extended Kalman filter," *IEEE Trans. Ind. Electron.*, vol. 67, no. 7, pp. 5971–5979, Jul. 2020.
[68] V. Smidl and Z. Peroutka, "Advantages of square-root extended Kalman filter for sensorless control of AC drives," *IEEE Trans. Ind. Electron.*, vol. 59, no. 11, pp. 4189–4196, Nov. 2012.
[69] S. Bolognani, L. Tubiana, and M. Zigliotto, "EKF-based sensorless IPM synchronous motor drive for flux-weakening applications," *IEEE Trans. Ind. Appl.*, vol. 39, no. 3, pp. 768–775, May 2003.
[70] S. Bolognani, R. Oboe, and M. Zigliotto, "Sensorless full-digital PMSM drive with EKF estimation of speed and rotor position," *IEEE Trans. Ind. Electron.*, vol. 46, no. 1, pp. 184–191, Feb. 1999.
[71] G. H. B. Foo, X. Zhang, and D. M. Vilathgamuwa, "A sensor fault detection and isolation method in interior permanent-magnet synchronous motor drives based on an extended Kalman filter," *IEEE Trans. Ind. Electron.*, vol. 60, no. 8, pp. 3485–3495, Aug. 2013.
[72] Z. Yin, F. Gao, Y. Zhang, C. Du, G. Li, and X. Sun, "A review of nonlinear Kalman filter appling to sensorless control for AC motor drives," *CES Trans. Electr. Mach. Syst.*, vol. 3, no. 4, pp. 351–362, Dec. 2019.
[73] T. Bernardes, V. F. Montagner, H. A. Gründling, and H. Pinheiro, "Discrete-time sliding mode observer for sensorless vector control of permanent magnet synchronous machine," *IEEE Trans. Ind. Electron.*, vol. 61, no. 4, pp. 1679–1691, Apr. 2014.
[74] G. Wang, Z. Li, G. Zhang, Y. Yu, and D. Xu, "Quadrature PLL-based high-order sliding-mode observer for IPMSM sensorless control with online MTPA control strategy," *IEEE Trans. Energy Convers.*, vol. 28, no. 1, pp. 214–224, Mar. 2013.
[75] H. A. A. Awan, T. Tuovinen, S. E. Saarakkala, and M. Hinkkanen, "Discrete-time observer design for sensorless synchronous motor drives," *IEEE Trans. Ind. Appl.*, vol. 52, no. 5, pp. 3968–3979, Sep. 2016.
[76] S.-C. Yang and G.-R. Chen, "High-speed position-sensorless drive of permanent-magnet machine using discrete-time EMF estimation," *IEEE Trans. Ind. Electron.*, vol. 64, no. 6, pp. 4444–4453, Jun. 2017.
[77] Y. Liang, D. Liang, S. Jia, S. Chu, and Y. Liang, "Robust DC-link voltage control and discrete-time sensorless control for high-speed flywheel energy storage system," in *Proc. Int. Conf. Electr. Mach. (ICEM)*, Aug. 2020, pp. 2457–2463.
[78] G.-R. Chen, S.-C. Yang, Y.-L. Hsu, and K. Li, "Position and speed estimation of permanent magnet machine sensorless drive at high speed using an improved phase-locked loop," *Energies*, vol. 10, no. 10, p. 1571, Oct. 2017.
[79] G. Zhang, G. Wang, D. Xu, and Y. Yu, "Discrete-time low-frequency-ratio synchronous-frame full-order observer for position sensorless IPMSM drives," *IEEE J. Emerg. Sel. Topics Power Electron.*, vol. 5, no. 2, pp. 870–879, Jun. 2017.
[80] Y. Yao, Y. Huang, and F. Peng, "Position sensorless drive of high speed permanent magnet synchronous motor," in *Proc. IEEE Energy Convers. Congr. Expo. (ECCE)*, Sep. 2018, pp. 1733–1740.
[81] Q. An, J. Zhang, Q. An, and A. Shamekov, "Quasi-proportional-resonant controller based adaptive position observer for sensorless control of PMSM drives under low carrier ratio," *IEEE Trans. Ind. Electron.*, vol. 67, no. 4, pp. 2564–2573, Apr. 2020.
[82] L. Ding, Y. Wei Li, N. R. Zargari, and R. Paes, "Sensorless control of CSC-fed PMSM drives with low switching frequency for electrical submersible pump application," *IEEE Trans. Ind. Appl.*, vol. 56, no. 4, pp. 3799–3808, Aug. 2020.
[83] M. L. Corradini, G. Ippoliti, G. Orlando, and S. Pettinari, "Speed estimation and fault detection for PMSM via quasi sliding modes," *IFAC Proc. Volumes*, vol. 44, no. 1, pp. 6142–6147, Jan. 2011.
[84] D. Xiao, S. Nalakath, S. R. Filho, G. Fang, A. Dong, Y. Sun, J. Wiseman, and A. Emadi, "Universal full-speed sensorless control scheme for interior permanent magnet synchronous motors," *IEEE Trans. Power Electron.*, vol. 36, no. 4, pp. 4723–4737, Apr. 2021.
[85] Z. Xia, S. R. Filho, D. Xiao, G. Fang, Y. Sun, J. Wiseman, and A. Emadi, "Computation-efficient online optimal tracking method for permanent magnet synchronous machine drives for MTPA and flux-weakening operations," *IEEE J. Emerg. Sel. Topics Power Electron.*, early access, Nov. 19, 2020, doi: 10.1109/JESTPE.2020.3039205.
[86] S. Bolognani, L. Ortombina, F. Tinazzi, and M. Zigliotto, "Model sensitivity of fundamental-frequency-based position estimators for sensorless pm and reluctance synchronous motor drives," *IEEE Trans. Ind. Electron.*, vol. 65, no. 1, pp. 77–85, Jan. 2018.
[87] M. S. Rafaq and J.-W. Jung, "A comprehensive review of state-of-the-art parameter estimation techniques for permanent magnet synchronous motors in wide speed range," *IEEE Trans. Ind. Informat.*, vol. 16, no. 7, pp. 4747–4758, Jul. 2020.
[88] Q. Wang, G. Zhang, G. Wang, C. Li, and D. Xu, "Offline parameter self-learning method for general-purpose PMSM drives with estimation error compensation," *IEEE Trans. Power Electron.*, vol. 34, no. 11, pp. 11103–11115, Nov. 2019.

[89] S. Ichikawa, M. Tomita, S. Doki, and S. Okuma, "Sensorless control of permanent-magnet synchronous motors using online parameter identification based on system identification theory," *IEEE Trans. Ind. Electron.*, vol. 53, no. 2, pp. 363–372, Apr. 2006.
[90] Y. Inoue, Y. Kawaguchi, S. Morimoto, and M. Sanada, "Performance improvement of sensorless IPMSM drives in a low-speed region using online parameter identification," *IEEE Trans. Ind. Appl.*, vol. 47, no. 2, pp. 798–804, Mar. 2011.
[91] Y. Inoue, K. Yamada, S. Morimoto, and M. Sanada, "Effectiveness of voltage error compensation and parameter identification for model-based sensorless control of IPMSM," *IEEE Trans. Ind. Appl.*, vol. 45, no. 1, pp. 213–221, Jan. 2009.
[92] M. S. Rafaq, F. Mwasilu, J. Kim, H. H. Choi, and J.-W. Jung, "Online parameter identification for model-based sensorless control of interior permanent magnet synchronous machine," *IEEE Trans. Power Electron.*, vol. 32, no. 6, pp. 4631–4643, Jun. 2017.
[93] Y. Shi, K. Sun, L. Huang, and Y. Li, "Online identification of permanent magnet flux based on extended Kalman filter for IPMSM drive with position sensorless control," *IEEE Trans. Ind. Electron.*, vol. 59, no. 11, pp. 4169–4178, Nov. 2012.
[94] F. Auger, M. Hilairet, J. M. Guerrero, E. Monmasson, T. Orlowska-Kowalska, and S. Katsura, "Industrial applications of the Kalman filter: A review," *IEEE Trans. Ind. Electron.*, vol. 60, no. 12, pp. 5458–5471, Dec. 2013.
[95] Z. Q. Zhu, X. Zhu, P. D. Sun, and D. Howe, "Estimation of winding resistance and PM flux-linkage in brushless AC machines by reduced-order extended Kalman filter," in *Proc. IEEE Int. Conf. Netw., Sens. Control*, Apr. 2007, pp. 740–745.
[96] Y. Yao, Y. Huang, F. Peng, and J. Dong, "Position sensorless drive and online parameter estimation for surface-mounted PMSMs based on adaptive full-state feedback control," *IEEE Trans. Power Electron.*, vol. 35, no. 7, pp. 7341–7355, Jul. 2020.
[97] B. Nahid-Mobarakeh, F. Meibody-Tabar, and F.-M. Sargos, "Mechanical sensorless control of PMSM with online estimation of stator resistance," *IEEE Trans. Ind. Appl.*, vol. 40, no. 2, pp. 457–471, Mar. 2004.
[98] M. Rashed, P. F. A. MacConnell, A. F. Stronach, and P. Acarnley, "Sensorless indirect-rotor-field-orientation speed control of a permanent-magnet synchronous motor with stator-resistance estimation," *IEEE Trans. Ind. Electron.*, vol. 54, no. 3, pp. 1664–1675, Jun. 2007.
[99] O. C. Kivanc and S. B. Ozturk, "Sensorless PMSM drive based on stator feedforward voltage estimation improved with MRAS multiparameter estimation," *IEEE/ASME Trans. Mechatronics*, vol. 23, no. 3, pp. 1326–1337, Jun. 2018.
[100] S. Ye and X. Yao, "A modified flux sliding-mode observer for the sensorless control of PMSMs with online stator resistance and inductance estimation," *IEEE Trans. Power Electron.*, vol. 35, no. 8, pp. 8652–8662, Aug. 2020.
[101] H. Lee and J. Lee, "Design of iterative sliding mode observer for sensorless PMSM control," *IEEE Trans. Control Syst. Technol.*, vol. 21, no. 4, pp. 1394–1399, Jul. 2013.
[102] T. Wang, J. Huang, M. Ye, J. Chen, W. Kong, M. Kang, and M. Yu, "An EMF observer for PMSM sensorless drives adaptive to stator resistance and rotor flux linkage," *IEEE J. Emerg. Sel. Topics Power Electron.*, vol. 7, no. 3, pp. 1899–1913, Sep. 2019.
[103] L. Colombo, M. L. Corradini, A. Cristofaro, G. Ippoliti, and G. Orlando, "An embedded strategy for online identification of PMSM parameters and sensorless control," *IEEE Trans. Control Syst. Technol.*, vol. 27, no. 6, pp. 2444–2452, Nov. 2019.
[104] C. Wu, Y. Zhao, and M. Sun, "Enhancing low-speed sensorless control of PMSM using phase voltage measurements and online multiple parameter identification," *IEEE Trans. Power Electron.*, vol. 35, no. 10, pp. 10700–10710, Oct. 2020.
[105] G. Wang, R. Yang, and D. Xu, "DSP-based control of sensorless IPMSM drives for wide-speed-range operation," *IEEE Trans. Ind. Electron.*, vol. 60, no. 2, pp. 720–727, Feb. 2013.
[106] C. Gong, Y. Hu, J. Gao, Y. Wang, and L. Yan, "An improved delay-suppressed sliding-mode observer for sensorless vector-controlled PMSM," *IEEE Trans. Ind. Electron.*, vol. 67, no. 7, pp. 5913–5923, Jul. 2020.
[107] S.-C. Yang and Y.-L. Hsu, "Full speed region sensorless drive of permanent-magnet machine combining saliency-based and back-EMF-based drive," *IEEE Trans. Ind. Electron.*, vol. 64, no. 2, pp. 1092–1101, Feb. 2017.
[108] G. Zhu, A. Kaddouri, L. A. Dessaint, and O. Akhrif, "A nonlinear state observer for the sensorless control of a permanent-magnet AC machine," *IEEE Trans. Ind. Electron.*, vol. 48, no. 6, pp. 1098–1108, Dec. 2001.
[109] J. Solsona, M. I. Valla, and C. Muravchik, "Nonlinear control of a permanent magnet synchronous motor with disturbance torque estimation," *IEEE Trans. Energy Convers.*, vol. 15, no. 2, pp. 163–168, Jun. 2000.
[110] J. Solsona, M. I. Valla, and C. Muravchik, "A nonlinear reduced order observer for permanent magnet synchronous motors," *IEEE Trans. Ind. Electron.*, vol. 43, no. 4, pp. 492–497, Aug. 1996.
[111] L. Qu, W. Qiao, and L. Qu, "An enhanced linear active disturbance rejection rotor position sensorless control for permanent magnet synchronous motors," *IEEE Trans. Power Electron.*, vol. 35, no. 6, pp. 6175–6184, Jun. 2020.
[112] R. W. Hejny and R. D. Lorenz, "Evaluating the practical low-speed limits for back-EMF tracking-based sensorless speed control using drive stiffness as a key metric," *IEEE Trans. Ind. Appl.*, vol. 47, no. 3, pp. 1337–1343, May 2011.
[113] D. Xiao, S. Nalakath, Y. Sun, J. Wiseman, and A. Emadi, "Complex-coefficient adaptive disturbance observer for position estimation of IPMSMs with robustness to DC errors," *IEEE Trans. Ind. Electron.*, vol. 67, no. 7, pp. 5924–5935, Jul. 2020.
[114] W. Xu, Y. Jiang, C. Mu, and F. Blaabjerg, "Improved nonlinear flux observer-based second-order SOIFO for PMSM sensorless control," *IEEE Trans. Power Electron.*, vol. 34, no. 1, pp. 565–579, Jan. 2019.
[115] Y. Jiang, W. Xu, C. Mu, J. Zhu, and R. Dian, "An improved third-order generalized integral flux observer for sensorless drive of PMSMs," *IEEE Trans. Ind. Electron.*, vol. 66, no. 12, pp. 9149–9160, Dec. 2019.
[116] J. Lu, Y. Hu, J. Liu, K. Ni, and H. Wen, "Detrimental effect elimination of current sensor accuracy uncertainty for high-precision position sensorless control of interior permanent magnet synchronous motor drives," *IEEE Trans. Ind. Electron.*, vol. 67, no. 7, pp. 6101–6111, Jul. 2020.
[117] J. Choi, K. Nam, A. A. Bobtsov, A. Pyrkin, and R. Ortega, "Robust adaptive sensorless control for permanent-magnet synchronous motors," *IEEE Trans. Power Electron.*, vol. 32, no. 5, pp. 3989–3997, May 2017.
[118] G. Wang, L. Ding, Z. Li, J. Xu, G. Zhang, H. Zhan, R. Ni, and D. Xu, "Enhanced position observer using second-order generalized integrator for sensorless interior permanent magnet synchronous motor drives," *IEEE Trans. Energy Convers.*, vol. 29, no. 2, pp. 486–495, Jun. 2014.
[119] D. Kim, Y.-C. Kwon, S.-K. Sul, J.-H. Kim, and R.-S. Yu, "Suppression of injection voltage disturbance for high-frequency square-wave injection sensorless drive with regulation of induced high-frequency current ripple," *IEEE Trans. Ind. Appl.*, vol. 52, no. 1, pp. 302–312, Jan. 2016.
[120] P. Hutterer, H. Grabner, S. Silber, W. Amrhein, and W. Schaefer, "A study on systematic errors concerning rotor position estimation of PMSM based on back EMF voltage observation," in *Proc. IEEE Int. Electric Mach. Drives Conf.*, May 2009, pp. 1393–1400.
[121] X. Wang, S. Nalakath, S. Filho, G. Zhao, Y. Sun, J. Wiseman, and A. Emadi, "A simple and effective compensation method for inverter nonlinearity," in *Proc. IEEE Transp. Electrific. Conf. Expo (ITEC)*, Jun. 2020, pp. 638–643.
[122] B. Wu and M. Narimani, "Two-level voltage source inverter," in *High-Power Converters and AC Drives*. Piscataway, NJ, USA: Wiley, 2017, pp. 93–117.
[123] Y. Jiang, W. Xu, and C. Mu, "Improved SOIFO-based rotor flux observer for PMSM sensorless control," in *Proc. IECON 43rd Annu. Conf. IEEE Ind. Electron. Soc.*, Oct. 2017, pp. 8219–8224.
[124] T. Chen, S. Huang, X. Wu, and T. Wu, "Improved-reduced order generalized integrator based sliding-mode observer for interior permanent magnet synchronous motor sensorless control," in *Proc. 22nd Int. Conf. Electr. Mach. Syst., (ICEMS)*, Aug. 2019, pp. 1–6.
[125] J. Ji, Y. Jiang, W. Zhao, Q. Chen, and A. Yang, "Sensorless control of linear Vernier permanent-magnet motor based on improved mover flux observer," *IEEE Trans. Power Electron.*, vol. 35, no. 4, pp. 3869–3877, Apr. 2020.
[126] Y. Wang, Y. Xu, and J. Zou, "Sliding-mode sensorless control of PMSM with inverter nonlinearity compensation," *IEEE Trans. Power Electron.*, vol. 34, no. 10, pp. 10206–10220, Oct. 2019.
[127] D. Bao, X. Pan, Y. Wang, X. Wang, and K. Li, "Adaptive synchronous-frequency tracking-mode observer for the sensorless control of a surface PMSM," *IEEE Trans. Ind. Appl.*, vol. 54, no. 6, pp. 6460–6471, Nov. 2018.
[128] S. Golestan, J. M. Guerrero, and G. B. Gharehpetian, "Five approaches to deal with problem of DC offset in phase-locked loop algorithms: Design considerations and performance evaluations," *IEEE Trans. Power Electron.*, vol. 31, no. 1, pp. 648–661, Jan. 2016.

[129] S. Golestan, J. M. Guerrero, F. Musavi, and J. C. Vasquez, "Single-phase frequency-locked loops: A comprehensive review," *IEEE Trans. Power Electron.*, vol. 34, no. 12, pp. 11791–11812, Dec. 2019.
[130] S. Golestan, S. Y. Mousazadeh, J. M. Guerrero, and J. C. Vasquez, "A critical examination of frequency-fixed second-order generalized integrator-based phase-locked loops," *IEEE Trans. Power Electron.*, vol. 32, no. 9, pp. 6666–6672, Sep. 2017.
[131] S. Golestan, J. M. Guerrero, J. C. Vasquez, A. M. Abusorrah, and Y. Al-Turki, "Modeling, tuning, and performance comparison of second-order-generalized-integrator-based FLLs," *IEEE Trans. Power Electron.*, vol. 33, no. 12, pp. 10229–10239, Dec. 2018.
[132] S. Gude, C.-C. Chu, and S. V. Vedula, "Recursive implementation of multiple delayed signal cancellation operators and their applications in prefiltered and in-loop filtered PLLs under adverse grid conditions," *IEEE Trans. Ind. Appl.*, vol. 55, no. 5, pp. 5383–5394, Sep. 2019.
[133] M. Ramezani, S. Golestan, S. Li, and J. M. Guerrero, "A simple approach to enhance the performance of complex-coefficient filter-based PLL in grid-connected applications," *IEEE Trans. Ind. Electron.*, vol. 65, no. 6, pp. 5081–5085, Jun. 2018.
[134] G. Zhang, G. Wang, D. Xu, and N. Zhao, "ADALINE-network-based PLL for position sensorless interior permanent magnet synchronous motor drives," *IEEE Trans. Power Electron.*, vol. 31, no. 2, pp. 1450–1460, Feb. 2016.
[135] G. Zhang, G. Wang, D. Xu, R. Ni, and C. Jia, "Multiple-AVF cross-feedback-network-based position error harmonic fluctuation elimination for sensorless IPMSM drives," *IEEE Trans. Ind. Electron.*, vol. 63, no. 2, pp. 821–831, Feb. 2016.
[136] G. Wang, T. Li, G. Zhang, X. Gui, and D. Xu, "Position estimation error reduction using recursive-least-square adaptive filter for model-based sensorless interior permanent-magnet synchronous motor drives," *IEEE Trans. Ind. Electron.*, vol. 61, no. 9, pp. 5115–5125, Sep. 2014.
[137] G. Wang, H. Zhan, G. Zhang, X. Gui, and D. Xu, "Adaptive compensation method of position estimation harmonic error for EMF-based observer in sensorless IPMSM drives," *IEEE Trans. Power Electron.*, vol. 29, no. 6, pp. 3055–3064, Jun. 2014.
[138] X. Wu, S. Huang, K. Liu, K. Lu, Y. Hu, W. Pan, and X. Peng, "Enhanced position sensorless control using bilinear recursive least squares adaptive filter for interior permanent magnet synchronous motor," *IEEE Trans. Power Electron.*, vol. 35, no. 1, pp. 681–698, Jan. 2020.
[139] D. Xiao, S. Nalakath, Z. Xia, G. Fang, Y. Sun, J. Wiseman, and A. Emadi, "Computation-efficient position estimation algorithm for permanent magnet synchronous motor drives under distorted conditions," *IEEE J. Emerg. Sel. Topics Power Electron.*, early access, May 4, 2020, doi: 10.1109/JESTPE.2020.2992243.
[140] Y. Wang, Y. Xu, and J. Zou, "ILC-based voltage compensation method for PMSM sensorless control considering inverter nonlinearity and sampling current DC bias," *IEEE Trans. Ind. Electron.*, vol. 67, no. 7, pp. 5980–5989, Jul. 2020.
[141] F. Tedesco, A. Casavola, and G. Fedele, "Unbiased estimation of sinusoidal signal parameters via discrete-time frequency-locked-loop filters," *IEEE Trans. Autom. Control*, vol. 62, no. 3, pp. 1484–1490, Mar. 2017.

CESAR JOSÉ VOLPATO FILHO was born in Caxias do Sul, in 1994. He received the B.Sc. and M.Sc. degrees in electrical engineering from the Federal University of Santa Maria, Santa Maria, Brazil, in 2017 and 2018, respectively, where he is currently pursuing the Ph.D. degree in electrical engineering with the Power Electronics and Control Research Group.

His research interests include high performance electric motor drives and applied nonlinear control.

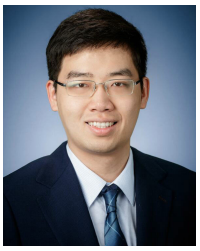

DIANXUN XIAO (Student Member, IEEE) received the B.Eng. and M.Eng. degrees in electrical engineering from the Harbin Institute of Technology, Harbin, China, in 2016 and 2018, respectively. He is currently pursuing the Ph.D. degree in electrical engineering with the McMaster Automotive Resource Centre, McMaster University, Hamilton, ON, Canada.

His current research interests include permanent magnet synchronous motor drives, switched reluctance motor drives, high-power converters, and battery management systems.

RODRIGO PADILHA VIEIRA (Member, IEEE) was born in Cruz Alta, Brazil. He received the B.S. degree in electrical engineering from the Universidade Regional do Noroeste do Estado do Rio Grande do Sul (Unijuí), Ijuí, Brazil, in 2007 and the M.Sc. and Dr. Eng. degrees in electrical engineering from the Federal University of Santa Maria (UFSM), Santa Maria, Brazil, in 2008 and 2012, respectively.

From 2010 to 2014, he was with the Federal University of Pampa, Alegrete, Brazil. Since 2014, he has been with the UFSM, where he is currently a Professor. His research interests include electrical machine drives, sensorless drives, and digital control techniques of static converters and energy systems.

ALI EMADI (Fellow, IEEE) received the B.S. and M.S. degrees (Hons.) in electrical engineering with from the Sharif University of Technology, Tehran, Iran, in 1995 and 1997, respectively, and the Ph.D. degree in electrical engineering from Texas A&M University, College Station, TX, USA, in 2000. He was the Founder, the Chairman, and the President of Hybrid Electric Vehicle Technologies, Inc. (HEVT)–a university spin-off company of Illinois Tech. He is also the President and the Chief Executive Officer of Enedym Inc. and Menlolab Inc.—two McMaster University spin-off companies. He is currently the Canada Excellence Research Chair Laureate with McMaster University, Hamilton, ON, Canada. He is also the holder of the NSERC/FCA Industrial Research Chair in electrified powertrains and a Tier I Canada Research Chair in transportation electrification and smart mobility. Before joining McMaster University, he was the Harris Perlstein Endowed Chair Professor of Engineering and the Director of the Electric Power and Power Electronics Center and the Grainger Laboratories, Illinois Institute of Technology, Chicago, where he established research and teaching facilities as well as courses in power electronics, motor drives, and vehicular power systems. He is the principal author or coauthor of over 500 journals and conference papers as well as several books, including *Vehicular Electric Power Systems* (2003), *Energy Efficient Electric Motors* (2004), *Uninterruptible Power Supplies and Active Filters* (2004), *Modern Electric, Hybrid Electric, and Fuel Cell Vehicles* (2nd Edition, 2009), and *Integrated Power Electronic Converters and Digital Control* (2009). He was the Inaugural General Chair of the 2012 IEEE Transportation Electrification Conference and Expo (ITEC). He chaired several IEEE and SAE conferences in the areas of vehicle power and propulsion. From 2014 to 2020, he was the Founding Editor-in-Chief of the IEEE TRANSACTIONS ON TRANSPORTATION ELECTRIFICATION. He is also an Editor of the *Handbook of Automotive Power Electronics and Motor Drives* (2005) and *Advanced Electric Drive Vehicles* (2014). He is also the Co-Editor of the *Switched Reluctance Motor Drives* (2018).